Westinghouse ENGINEER March 1968

Special Railroad Car Transports Generators Assembled

A railroad car that can manipulate its midsection like some ponderous slow-motion belly dancer is being used to transport electrical generators from the manufacturing plant at East Pittsburgh to the sites of power stations. The generator in the photograph was enroute to the St. Clair generating plant of Detroit Edison Company at St. Clair, Michigan.

The car's capacity is 1,046,000 pounds, it is 159 feet long when loaded, and it rides on 40 wheels. It was built for Westinghouse by McDowell-Wellman Engineering Company, Cleveland, Ohio.

The car is composed of two separate sections. In use, a generator is suspended between the sections and, partially supported by a pair of steel girders, becomes an integral part of the car. After the generator is unloaded, the two sections are hooked together for the return trip.

The car's "wiggle" is provided by a hydraulic system that can move the generator-girder assembly vertically and laterally to get over, under, and around obstructions along a railroad right-of-way. A generator can be shifted 14 inches sideways in about a minute, and 12 inches vertically in about five minutes.

Moreover, the car can carry a generator only six inches above the rails, in contrast to the 30-inch minimum clearance for conventional heavy-duty rolling stock. That feature permits shipping larger generators assembled without encountering height restrictions. Although some of the generators now on order will exceed even the new car's weight capacity, they can be shipped in just two pieces—rotor and stator—to reduce installation and delivery time.

Westinghouse ENGINEER
March 1968, Volume 28, Number 2

Subscriptions: United States and possessions, $2.50 per year; all other countries, $3.00 per year. Single copies, 50¢ each.

Mailing address: Westinghouse ENGINEER, P. O. Box 2278, 3 Gateway Center, Pittsburgh, Pennsylvania 15230.

Published bimonthly by the Westinghouse Electric Corporation, Pittsburgh, Pennsylvania. Printed in the United States by The Lakeside Press, Lancaster, Pennsylvania. Reproductions of the magazine by years are available on positive microfilm from University Microfilms, Inc., 300 North Zeeb Road, Ann Arbor, Michigan 48106.

Cover design: The ac motor is made in such a variety of types and sizes that a number of factors need to be considered in choosing a motor that will do the job and still be economical in first cost and operating cost. The article beginning on the next page discusses those factors, and the cover design by Tom Ruddy symbolizes the great variety in ac motors.

Selecting AC Motors for Economy with Capability

Carl R. Olson
E. S. McKelvy

Proper motor selection provides economies both in first cost and in operating cost. The savings opportunities are increased by recent advances in technology and changes in standards.

The most important factors to consider in selecting a motor are the adequacy of the motor for the application and the reliability of the motor. Once those requirements have been met, cost is a major consideration. The cost of a motor consists of two parts—its first cost and its operating cost—and both parts are affected by such variables as horsepower, voltage, motor type, insulation, and enclosure.

Improper selection can make both first cost and operating cost unnecessarily high. For example, oversize motors are often bought, either because the actual load requirements are not known or because of anticipated load growth. The latter reason may be economically justifiable; the former is not. The oversize motor not only costs more to begin with than a job-rated motor, it also costs more to operate. Motors perform best (maximum efficiency and power factor) at their nameplate ratings. The best checks against improper size are careful review of drive requirements before buying and periodic checks of the motor in operation.

Selection of insulation and enclosure also requires serious attention. Many improvements in both have been made recently; they often permit, for example, use of a less expensive weather-protected motor located outdoors in place of an explosion-proof or force-ventilated motor indoors in a potentially explosive atmosphere. For such reasons, it is important to review purchasing practices to make sure they are based on today's motor designs.

Also, the purchaser should review the motor requirements and specifications to make sure that all special features (such as nonstandard bearings and mounting dimensions) have been eliminated unless they serve some essential purpose. Many special features are specified merely because of an isolated case of trouble years ago; others may have been obsoleted by changes in manufacturing techniques.

Modern technology has reduced the size of motors, increased their expected life, and improved their resistance to dirt, moisture, and corrosion. The most significant change is the reduction in price in the face of continued inflation (Fig. 1a). Other important developments of the past 10 years are brushless excitation for synchronous motors and new two-speed single-winding induction motors. These results of modern technology are discussed in this article to help the motor user select motors and to help him understand the reasons for (and the value of) recent changes in designs and standards. The price curves presented reflect the latest changes in motor size, temperature standards, and motor design at the time of writing.

Price Estimating

Motor prices, on the basis of horsepower rating, are presented in Figs. 1 and 2. The curves are approximate only, but they are useful for preliminary price estimates and comparison purposes. They are based on published list prices and discounts for large user customers, such as typical petroleum and chemical companies. Fig. 1 is for standard basic motors, "Open" or "Open, Drip-proof" construction, in the voltage rating that results in lowest cost. Fig. 2 modifies these basic prices for different voltages and enclosures.

Synchronous and induction motors cannot always be compared on an equal-speed basis. In geared applications, the most economical induction motor speed is usually 1800 r/min; the most economical synchronous motor speed for the same application might be 900 or 1200 r/min, depending on the horsepower required. Thus, motor prices must not be compared directly speed for speed and horsepower for horsepower; they must be studied with the "whole job" concept.

In considering motors for any large drive (above 5000 hp), the motor manufacturer should be consulted early. Those machines are always custom designed for the specific application, taking into consideration the driven machine characteristics and the power system parameters and limitations. If the motor manufacturer can confer early with the machinery builder and utility system engineers, he can find the optimum drive-system solution.

Voltage—The effects of various voltages on the cost of motors is illustrated in Fig. 2a and 2b. Below 200 hp, the least expensive motors are low voltage (less than 600 volts). Above 500 hp and up to 5000 hp, 2300 volts can be considered standard. Above 5000 hp, the standard voltage is 4000 or 4160 volts. (More space is available for insulation in larger motors, so it is economically practical to use higher-voltage motors and control.)

As the size of a plant increases, its distribution system also increases, making higher system voltages desirable or necessary. For distribution system voltages above 5000 volts, the usual practice has been to transform down to 2400 or 4160 volts for large motors. Now, however, cable and transformer costs frequently make motors with higher voltages such as 13.8 kV economical. Many 11- to 14-kV motors are in service even outdoors.

Most motors below 200 hp are best supplied at the lower standard voltages of 230 or 460 volts. (Winding reliability is lowered by selecting higher voltages for the lower horsepowers, such as 2300 volts for 150 hp and below or 4160 volts for 200 hp and below.) Motor voltage standards have been changed recently from 110, 220, 440, and 550 to a suggested standard for future designs (to which most motors are now being built) of 115, 230, 460, and 575 volts. The new motor voltages are

1—Approximate prices for ac motors as of November 1967. (The curves in Figs. 1 and 2 have been smoothed for readability; actual curves would have discontinuities because of jumps in frame size and other irregularities.) (*a*) Squirrel-cage induction motors, three-phase 60-Hz, with standard voltages and "Open, Drip-proof" enclosures. To indicate how prices have decreased in recent years, the top curve shows prices of 1800-r/min motors in 1958. (*b*) Conventional synchronous motors (with slip rings), three-phase 60-Hz, with standard voltages and "Open, Drip-proof" or "Open" enclosures. (*c*) Brushless synchronous motors, three-phase 60-Hz, with standard "Open, Drip-proof" or "Open" enclosures.

Carl R. Olson and E. S. McKelvy are applications engineers in Industrial Projects Marketing, Westinghouse Electric Corporation, Pittsburgh, Pennsylvania.

a

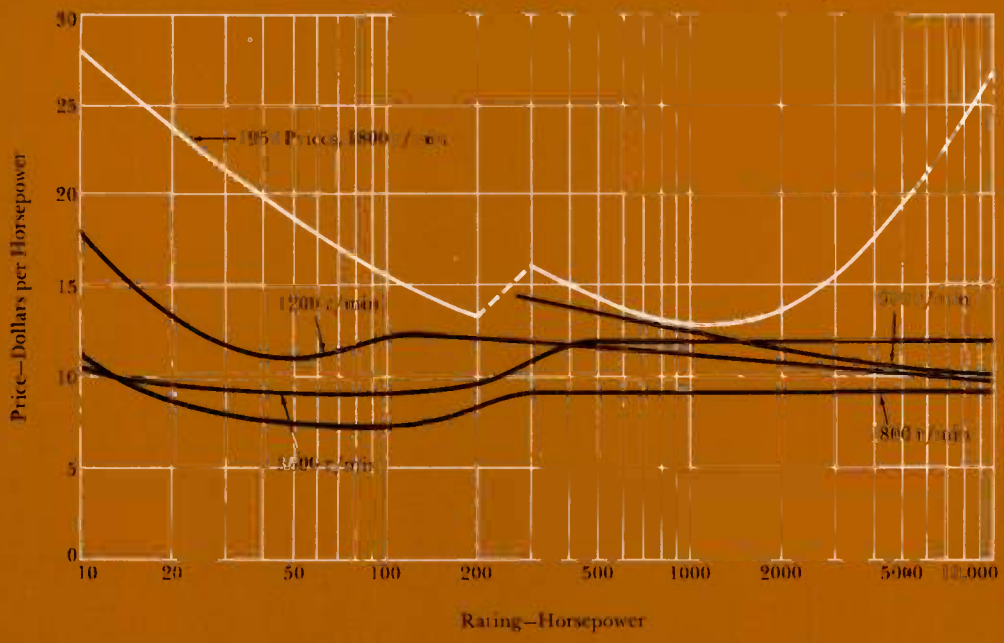

b

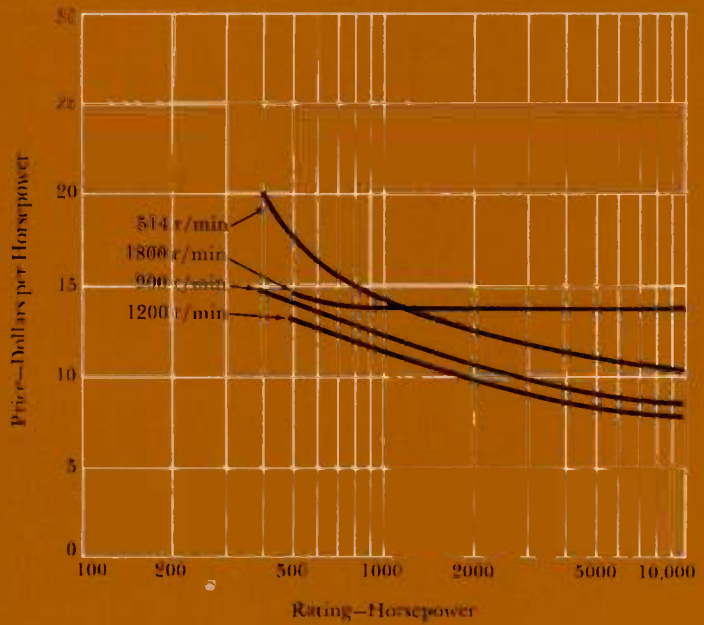

c

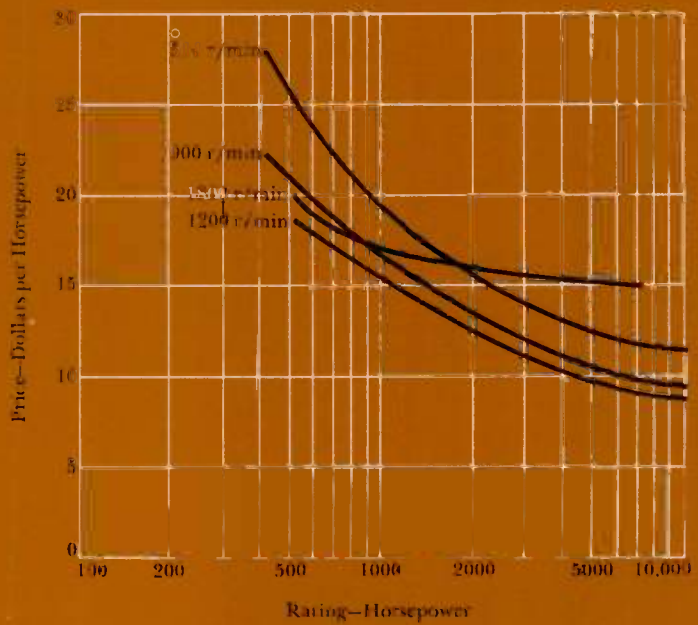

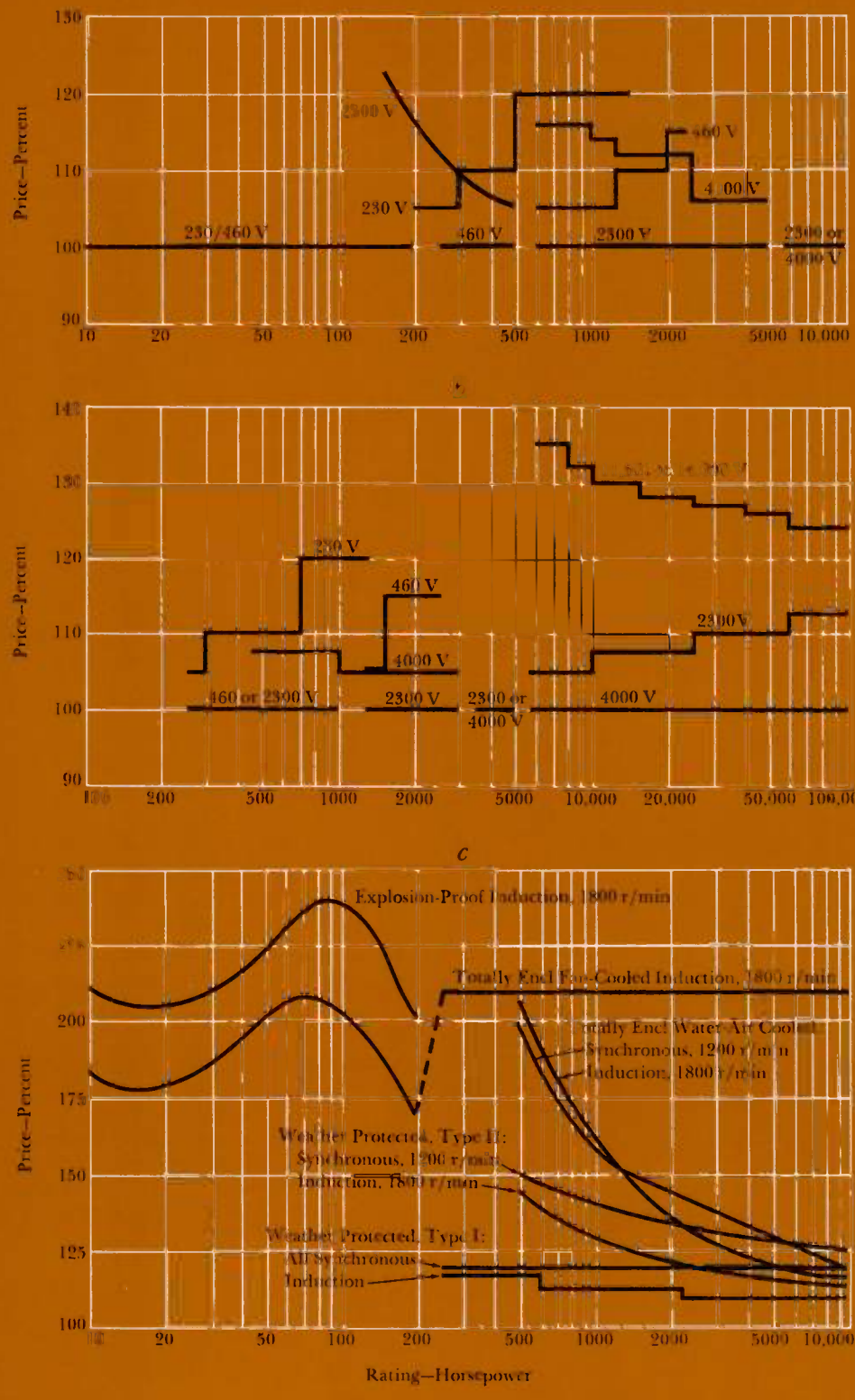

2—Voltage rating and enclosure type affect the cost of ac motors. Curves read from left to right; at steps, use the first value reached. (*a*) Effect of voltage rating on cost of squirrel-cage induction motors. Percentages refer to the base prices shown in Fig. 1*a*. (*b*) Effect of voltage rating on cost of synchronous motors. Percentages refer to the base prices shown in Figs. 1*b* and 1*c*. (*c*) Effect of enclosure type on costs of induction and synchronous motors. Percentages refer to Fig. 1 after applying Figs. 2*a* and *b*. The enclosures included here are the most common types.

closer to the voltages in modern stiff distribution systems nominally at 120, 240, 480, or 600 volts. In the past, 220-volt motors could be operated at their rated horsepower on 120/208-volt systems; the new 230-volt motors, however, are not designed to operate at their rated horsepower at 208 volts. This is an important consideration in office buildings and other locations where many motors are operated on 120/208-volt lighting systems. Motors designed specifically for 208 volts should be used if rated horsepower is expected.

Enclosures—The motor enclosure selected affects cost substantially (Fig. 2c). However, use of one of the special protective enclosures may be dictated by the atmosphere encountered.

Today's standard motor enclosure for induction and high-speed synchronous motors is the "Open, Drip-proof" (Fig. 3). The Westinghouse Life-Guard T motor combines the economy of drip-proof construction with the extra protection of stator insulation sealed to air or moisture. It is designed for critical applications where excessive moisture, oil, or corrosive fumes make ordinary drip-proof motors impractical. The complete motor insulation system is encapsulated with epoxy resin to seal the windings from air or moisture. Before the epoxy is applied, end turns are fortified with woven reinforcement to improve mechanical strength.

Open, Drip-proof construction for large motors is shown in Fig. 4. For still larger sizes, the "Fully Accessible" construction is used with squirrel-cage, synchronous, and wound-rotor motors; it is similar in appearance to that shown in Fig. 5.

The next degree of protection for the larger motors is "Weather Protected, Type I." Such a motor is defined as "an open machine with its ventilating passages so constructed as to minimize the entrance of rain, snow, and airborne particles to the electric parts."[1] All openings are restricted against passage of a rod of ¾-inch diameter. A few years ago, this type of motor could not have been used outdoors because the insulation available could not withstand the moisture and other deteriorating effects. With today's vacuum-pressure epoxy-impregnated insulation, it is often used outdoors.

Where a higher degree of protection and longer life are desired, "Weather Protected, Type II" motors are recommended for the large sizes (Fig. 5). They have extensive baffling of the ventilating system so that the air must turn at least three 90-degree corners before entering the active motor parts; thus, rain, snow, and dirt carried by driving winds are blown through the motor housing without entering the active parts.

"Totally Enclosed" motors offer the greatest protection against moisture, corrosive vapors, dust, and dirt. Totally enclosed fan-cooled (TEFC) motors are the obvious choice below 250 hp (Fig. 6). Their internal and external ventilating air are kept separate; external air never gets inside, except for the small amount that enters by "breathing."

Above 500 hp, enclosed motors with water-to-air coolers cost much less than TEFC motors; in large synchronous-motor ratings, they cost even less than Weather-Protected, Type II. Large enclosed synchronous machines with coolers for mounting in the motor foundation are frequently supplied at lower cost than the motors with integral-mounted coolers used as the reference in Fig. 2c.

Motors often must be applied in areas where there is a fire or explosion hazard. The hazards include explosive gases and vapors such as gasoline; dust such as coal, flour, or metals that can explode when suspended in air; and fibers such as textile lint. The kind of motor enclosure used depends on the type of hazard, type and size of motor, and probability of a hazardous condition occuring. Some of the kinds are: explosion-proof motors, which can withstand an internal explosion; force-ventilated motors ventilated with air from a safe location; and totally enclosed motors cooled by air-to-water heat exchangers and pressurized with safe air, instrument air, or inert gas.

Insulation

Electrical insulation is being improved every year, and motor manufacturers make use of this and other technological developments to put more power into smaller, lighter, more efficient packages. In 1956, for example, a 10-hp 1800-r/min motor was built on a 256 frame; today's standards call for 20 hp on that frame at the same speed.

The newest catalogs show standard induction motors designed with Class B insulation for operation in a 40 degrees C ambient with 80 degrees C rise by resistance at 100-percent load for motors with 1.0 service factor. Previously, induction motor ratings were based on temperature rise by thermometer. Catalogs for large synchronous motors still refer to temperature rise by thermometer.

These changes require an explanation. NEMA standards show three methods of temperature determination: thermometer, resistance, and embedded detector. Motor engineers have long recognized that measuring temperature rise by placing a thermometer against the end windings does not give the best indication of insulation temperatures near the conductors in the slots. Measuring temperature rise by resistance gives a better indication of temperature in the hottest part of the winding. Machines equipped with temperature detectors usually show a difference between readings taken by embedded detector and those taken by winding resistance, with the detector reading usually slightly higher. The standards, however, allow 80 degrees C rise by either method for stator windings with Class B insulation. Total temperature for any insulation system also depends on the equipment to which it is applied. For example, railway motors with Class B insulation have rated *standard* rises by resistance of 120 degrees C on the armature; induction motors with service factor have 90 degrees C rise at the service-factor load.

Service Factor

For many years, it was common practice to give standard open induction motors a 1.15 service factor rating; that is, the motor would operate at a safe temperature at 15 percent overload. That practice has changed for large motors, which are closely tailored to specific applications. [The term "large motors," as used in this section, includes synchronous motors, all

induction motors larger than 200 hp, and all induction motors with 16 or more poles (450 r/min at 60 Hz)].

The new catalogs for large induction motors are based on standard motors with Class B insulation of 80 degrees C rise by resistance, 1.0 service factor. Previously, they were 60 degrees C rise by thermometer, 1.15 service factor. This change is a case of catching up with the standards.

Service factor is nowhere mentioned in the NEMA standards for large machines; there is no definition of it and no standard for temperature rise or other characteristics at the service-factor overload.[1] In fact, the standards are being changed to state that the temperature-rise tables are for motors with 1.0 service factor. Neither standard synchronous nor enclosed induction motors have included service factor for several years.

Almost all large motors today are designed specifically for a particular application and for a specific driven machine. In sizing the motor for the load, horsepower is usually selected so that ad-

3

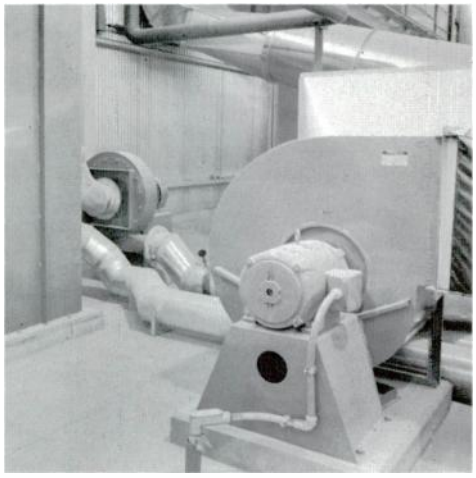

4

5

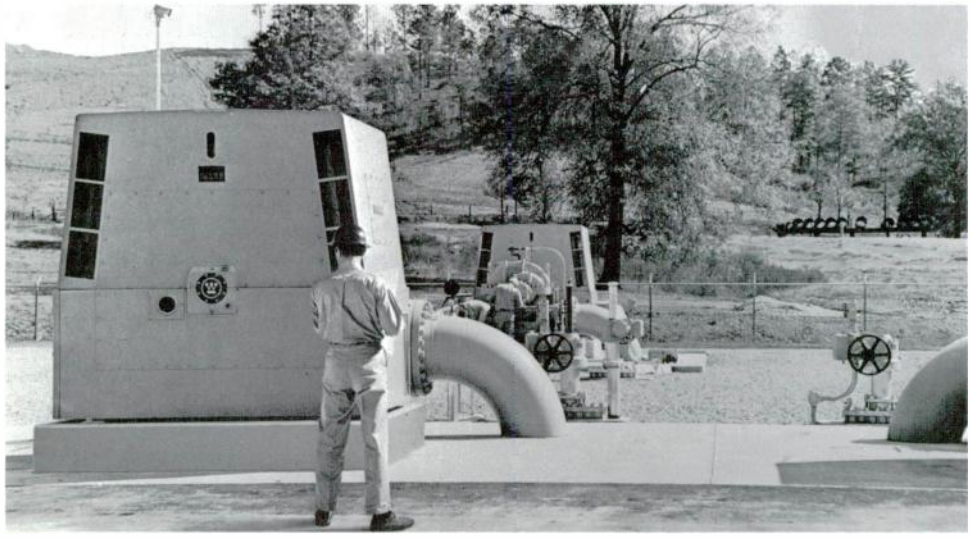

6

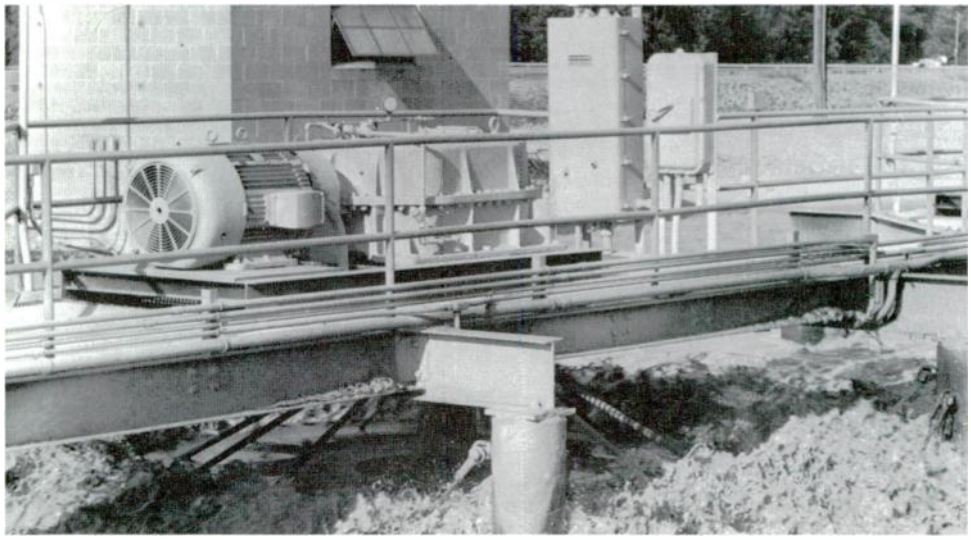

3—"Open, Drip-Proof" construction provides a high degree of protection, which can be increased with accessory screens and drip covers. This typical integral-horsepower motor drives a ventilating fan.

4—Modern insulation permits outdoor installation of "Open, Drip-proof" motors. The construction shown here is used for frames larger than 445U, through 1000-hp four-pole. "Weather Protected, Type I" construction is similar in appearance in these ratings, except for addition of screens to the ventilating openings.

5—Fully Accessible construction is used for "Open, Drip-proof," "Weather Protected, Type I," and "Weather Protected, Type II" motors from 1000 hp to about 20,000 hp. The top lifts off for inspection and maintenance. Many such motors are in service outdoors, as these 5000-hp "Weather Protected, Type II" motors that drive pipeline pumps.

6—Totally enclosed fan-cooled motors are protected against airborne contaminants by passing cooling air over outer ribs instead of through the active parts. (Explosion-proof motors are similar except for extra-heavy cast-iron conduit boxes with metal-to-metal fit, longer and closer tolerances on rabbet fits, and extra-long shaft collar flame paths.) This motor drives aeration equipment at a paper mill; it is located outdoors.

ditional overload capacity is not required; a purchaser should not be required to pay for capability he doesn't need. With the elimination of service factor, standard motor base prices have been reduced four to five percent to reflect the savings.

Purchasers should specify standard horsepower ratings, without service factor, for these reasons:

1) All of the larger standard horsepowers are within or close to 15-percent steps.

2) As stated in NEMA, the use of next larger horsepower prevents the exceeding of standard temperature rise.

3) The larger horsepower provides increased pull-out torque, starting torque, and pull-up torque.

4) The practice of using 1.0 service factor induction motors is consistent with that generally followed in selecting horsepower requirements of synchronous motors.

5) For loads requiring an occasional overload, such as start-up of a pump with cold water followed by continuous operation with hot water at lower horsepower loads, the motor probably should have a short-time overload rating.

Induction motors with 1.15 service factor are still available. Large open motors (except splash-proof) are available for an addition of five percent to the base price with a specified temperature rise of 90 degrees C for Class B insulation by resistance at the overload horsepower. This means the net price is approximately the same as before. The temperature rise at the 1.15 service factor horsepower was "within safe temperature;" now temperature rise at service factor horsepower is tied down. At nameplate power, the service-factor rated motor usually has less than 80 degrees C rise by resistance.

Motors with a higher service factor rating, such as 1.25, are also still available, but they must be specially designed and manufactured and are not normally justifiable. Most smaller open induction motors (200 hp and below, 514 r/min and above) still have the 1.15 service factor rating. Motors in that size range with 1.15 service factor are standard, general-purpose, single-speed continuous-rated, 60-Hz, design A or B, drip-proof machines. Those that normally have a service factor of 1.0 are totally enclosed motors, intermittent rated motors, high-slip design D motors, most multispeed motors, encapsulated motors, and motors other than 60 Hz.

Synchronous Motors

Synchronous motors have definite advantages of lower cost, higher efficiency, and better power factor in some applications. They are frequently used to drive reciprocating compressors, motor-generator sets, fans, pumps, and ball mills. They are also used for high-speed (above 3600 r/min) centrifugal compressor drives of several thousand horsepower.

One of the useful characteristics of synchronous motors is their ability to provide power factor correction for the electrical system. Standard synchronous motors are available rated either 100 or 80 percent leading power factor. At 80 percent power factor, 60 percent of the motor rated kVA is delivered to the system as reactive kVA for improving system power factor. This leading reactive kVA increases as load decreases; at zero load with rated field current, the leading reactive kVA is approximately 80 percent of the motor rated kVA. A machine with unity power factor does not provide any leading current at rated load. However, at reduced loads with constant field current, it operates at leading power factor; at zero load, the leading kVA is about 30 percent of motor rated kVA.

Because of their larger size, motors with 80 percent power factor cost 15 to 20 percent more than those with unity power factor, but their use still may be less expensive than an equivalent bank of capacitors. An advantage of using synchronous motors for power factor correction is that the reactive kVA can be varied at will by adjusting the field current. Synchronous motors, furthermore, generate more reactive kVA as the voltage decreases (for moderate dips); they therefore tend to stabilize system voltage better than capacitors, since they supply maximum leading kVA when the voltage is at a minimum.

When pull-out torques higher than standard are required, motors with leading power factor (80 percent) should be considered because they may be less expensive. The reason is that the easiest way to design for high pull-out is to provide additional flux, which causes leading power factor. In addition to power factor advantages, efficiency of synchronous motors is higher than that of similar induction motors. (See Table I.)

Direct-connected exciters are fairly common for general-purpose and large high-speed synchronous motors. At low speeds (514 r/min and below) the direct-connected exciter is large and expensive. Motor-generator sets and static (rectifier) exciters are widely used for low-speed synchronous motors and when a number of motors are supplied from a single excitation bus.

Brushless Excitation—One of the most significant developments in recent years is brushless excitation for synchronous machines. It became possible with the availability of reliable long-life solid-state control and power devices (diodes, transistors, and thyristors). Brushless excitation eliminates brushes, collector rings, and commutator from the motor and

Table I. Typical Full-Load Efficiencies of Large Induction and Synchronous Motors

HP	*3600 r/min*	*1200 r/min*	*600 r/min*	*300 r/min*
250	91.5	92.0	91.0	....
	....	93.9*	93.4*	92.8*
1000	94.2	93.7	93.5	92.3
	....	95.5*	95.5*	95.5*
5000	96.0	95.2	....	....
	....	....	97.2*	97.3*

*Synchronous motors with 1.0 power factor. Synchronous motors with leading power factors have efficiencies approximately 0.5 to 1.0 percent lower.

exciter, eliminating also the maintenance required by those components and permitting use of synchronous motors in many hazardous and corrosive areas where conventional motors could not be used without extensive additional protection. All the advantages of conventional synchronous motors are retained—constant speed, high efficiency, power-factor correction, and varied performance capability. The solid-state field application control is rotor mounted; it is precise and fast acting and provides the same full complement of functions as a conventional synchronizing panel.

The exciter is an ac generator with a stator-mounted field excited from an external dc source. Output of the exciter is converted to dc power through a three-phase full-wave silicon-diode bridge rectifier. Thyristors switch the current to the motor field and the motor-starting field-discharge resistors. These semiconductor elements are mounted on heat sinks and assembled on a drum bolted to the rotor or shaft. In the Westinghouse design, the field discharge resistors are bolted to the rotor spider in low-speed motors and mounted on the semiconductor drum in high-speed machines.

Semiconductor control modules gate the thyristors, which switch current to the motor field at the optimum motor speed and precise phase angle. This assures synchronizing and minimum system disturbance. On pull-out, the discharge resistor is reapplied and excitation removed to provide protection. The control resynchronizes the motor, after the cause of pull-out is removed, if sufficient torque is available. The field is automatically applied if the motor synchronizes on reluctance torque. The control is calibrated at the factory, and no subsequent adjustment is required. Optimum slip frequency at pull-in is based on total motor and load inertia. All control parts are interchangeable and can be replaced without affecting starting or running operation.

New Multispeed Motors

Since about the turn of the century, two-speed induction motors have been built with a 2:1 speed ratio from a single stator winding. Other speed ratios, however, required two separate stator windings until the principle of pole amplitude modulation (PAM) was formulated recently.[2] This new type of induction motor has been built in ratings as large as 3200 hp.

Many drive applications are ideally suited for the two-speed PAM motor, such as forced- or induced-draft boiler fans. Used with fans having vane control, the motor offers definite advantages over a combination of hydraulic coupling, motor, and fan. Other typical applications are ventilating fans, centrifugal pumps, compressors, and cooling-tower fans.

The two speeds are obtained with only one winding and any combination of pairs of poles (as 8/10 poles, 900/720 r/min, or as wide as 4/20 poles, 1800/360 r/min). PAM motors are smaller than equivalent two-winding machines and approximately 10 percent lighter. The entire winding works at both high and low speed, resulting in greater thermal capacity and higher efficiency. All coils have identical size and pitch, permitting efficient manufacturing. The motors require less active material and winding labor and therefore are lower in cost than two-winding machines. Torque, noise, and loss characteristics compare favorably with those of two-winding motors. (See Table II.)

The PAM approach is to modulate the stator flux field of an induction motor. It is based on the principle that if a signal of one frequency is acted on (modulated) by another frequency, the result is two new frequencies equal to the signal frequency plus and minus the modulating frequency. Thus, 60 Hz modulated by 2 Hz gives resultant frequencies of 58 and 62 Hz. Likewise, if a six-pole field is modulated by a two-pole field, the result is a four-pole field and an eight-pole field. Modulation is accomplished by reversing all the coils in half the periphery of the machine. If only a remaining eight-pole field is desired, the four-pole field can be eliminated by proper spacing of the starting point of each phase winding. Such a motor runs at six-pole speed when connected normally and at eight-pole speed when half the coils are reversed.

*Table II. Comparison of Two-Winding Induction Motor With PAM Motor**

	Two-Winding Motor	*PAM Motor*
Total Motor Weight	13,000 lb	11,000 lb
Weight of Largest Part	4900 lb	4300 lb
Dimensions of Largest Part	71 in.	63 in.
Motor Losses (maximum)		
High Speed	65.4 kW	60.1 kW
Low Speed	36.3 kW	31.6 kW
Relative Cost	1.00	0.75

*Two-winding 1200/600-hp 900/720-r/min motor compared with single-winding PAM motor operating at the same speeds.

Conclusion

Improved electrical insulations in the newer motors withstand heat, moisture, and corrosive atmospheres better than former ones; new metals can take mechanical punishment longer; and computer techniques optimize design.[3] These and other developments, and the resulting motor rerates, have dramatically increased the amount of motor in a given package. Because of the wide variety of motor types, materials, and ratings available, motor users need to select their motors carefully to take advantage of all the opportunities to minimize both first cost and operating cost.

References:
[1] *Motors and Generators*, Pub. No. MG1-1968, National Electrical Manufacturers Association, New York City.
[2] Robinson, R. C., "PAM Induction Motors—Two Speeds with One Winding," *Westinghouse ENGINEER*, Sept. 1967.
[3] Chen, H. M., Karr, F. R., and List, F. A., "Electrical Machines Improved Through a Decade of Design Progress with Computers," *Westinghouse ENGINEER*, July 1967.

Electron-Beam Welder for Use in Space

Harry G. Lienau
Jerald F. Lowry
C. B. Hassan

Metals probably will have to be joined in space to assemble and repair future space vehicles. One promising method is electron-beam welding. An experimental battery-powered welder has been developed in a program aimed at test welding in an orbiting workshop.

Thus far, the vehicles man has used for space exploration have been small enough to be lofted into orbit or toward their destinations by a single rocket vehicle. However, beyond the Apollo moon-landing program lie plans for more ambitious expeditions, and longer stays by men in earth orbit. Both require large vehicles or stations, which will have to be assembled from parts placed separately in earth orbit.

To assemble the parts, suitable metals-joining techniques will be needed. Accordingly, experiments to develop processes and supporting equipment for such techniques as welding, brazing, and use of mechanical fasteners are in progress or being considered in the National Aeronautics and Space Administration's Apollo Applications Program. The main purposes of the experiments are to determine the extent to which the joining methods can be used for fabrication and repair in space, and to enable future planners to develop and test processes and equipment at earth gravity with assurance of satisfactory performance at zero gravity.

Electron-beam welding probably has the greatest promise. The process is fairly well understood; it can be adapted readily to simplified control; it is applicable to a broad range of metals, including all those used in space-vehicle structures; and it is probably the most efficient welding process, in energy utilization, because of the steep thermal gradients resulting from the high energy densities used. The principal problem is the bulk and mass of the power-handling equipment; now that problem has been solved with development of a battery-operated, lightweight, portable, electron-beam welder by Westinghouse under contract to NASA. (The Westinghouse Astronuclear Laboratory is prime contractor on the project.)

The design, fabrication, and qualification program for the space experiment package is in progress at the Marshall Space Flight Center's Manufacturing Engineering Laboratory. The primary object of the experiment is to determine and attempt to understand the effects of weightlessness on the electron-beam welding process. Weightlessness presumably could cause the molten weld metal to "ball up" and float away, and spattering might damage both nearby and distant surfaces. The low ambient pressure also creates problems, such as possible evaporation of molten weld metal, control of joining temperatures, and waste heat dissipation. However, the hope is that these joining problems will be minimized by the steep thermal gradients and small melted zones characteristic of electron-beam welding. Moreover, the vacuum environment will facilitate volatilization of surface oxide films and help reduce recontamination of cleaned surfaces; both factors should contribute to the quality of the welds produced. Welds should be free of joining defects, and they should have high strength-to-weight ratios relative to the parent metal.

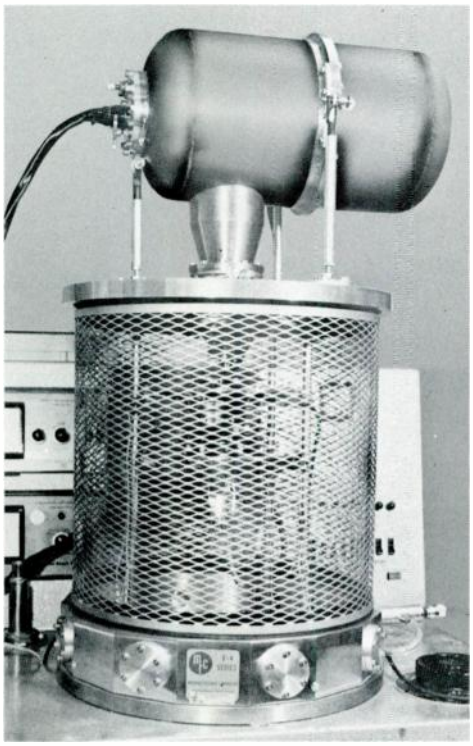

1—Laboratory model of the self-contained electron-beam welder is mounted on a vacuum system here for welding tests. It can operate on its batteries for about five minutes, producing high-quality welds in a wide variety of metals. The cable connects the welder to its control panel.

The experiment is designed to obtain as much useful information as possible as simply as possible. All performance parameters (such as welding speed and beam power) and most environmental conditions (such as temperature, vacuum, and radiation) will be duplicated in preflight tests. These parameters will be fixed during the flight experiment, leaving weightlessness the only unknown condition affecting quality of the weld specimens produced in space. Weld specimens, and motion pictures taken during the experiment, will be returned from orbit to compare the characteristics of welds made in space with those made in the laboratory under earth-gravity conditions and to formulate materials-joining criteria for design of space structures.

Laboratory Welder

The first welder built is a self-contained, battery-operated, two-kilowatt unit capable of producing a 20-kilovolt, 100-milliampere, tightly focused electron beam for about five minutes at a time (Fig. 1). It was intended for laboratory use—to aid in the design of the actual in-orbit welding experiment. The device is designed to be mounted on a glass or metal cylinder or placed inside a larger vacuum chamber. Either way, welding tests can then be performed in the evacuated chamber.

The complete unit consists of a sealed stainless-steel vessel containing the main battery pack, dc-to-dc converter, filament

Harry G. Lienau is a research and development engineer at NASA's Marshall Space Flight Center, Huntsville, Alabama. J. F. Lowry and C. B. Hassan are design and development engineers at the Research Laboratories, Westinghouse Electric Corporation, Pittsburgh, Pennsylvania.

This article was adapted from a paper presented by the authors at the IEEE Ninth Annual Symposium on Electron, Ion, and Laser Beam Technology, Berkeley, California, May 9-11, 1967.

battery pack, filament control circuit, and electron-beam gun; a keeper valve; and a magnetic lens attached to the pressure vessel (Fig. 2). An external rack-mounted control panel is connected by a cable to the pressure-vessel circuitry. The unit can be powered, via the cable, from an external source to conserve batteries. To permit small high-voltage clearances and thus minimize the size of the unit, the vessel is pressurized to 60 psia with sulfur hexafluoride (SF_6). The unit weighs 61 pounds and is 21 inches long by 12 inches in diameter, with the magnetic lens protruding 10 inches.

The main battery pack consists of 27 rechargeable silver-zinc batteries connected in series. Open-circuit voltage is about 50 volts; under the nominal 70-ampere load, battery voltage drops to 35 volts. When fully charged, the battery stores 525 watt-hours of energy.

The dc-to-dc converter has a rating of two kW; it consists of an inverter that converts the input dc power to ac power, a step-up transformer, and a high-voltage rectifier and filter. A transistor oscillator generates a square wave of approximately three kilohertz, which drives the two banks of power transistors in the inverter stage. Each bank is connected between one side of the center-tapped primary of the transformer and an aluminum base plate that acts as a mechanical support and heat sink for the oscillator and inverter components. This transformer center tap is connected to the positive terminal of the main battery; the negative battery terminal is connected to the base plate. The two transistor banks are alternately turned on and off, which, in effect, applies an alternating-voltage square wave across the primary winding of the transformer.

The high-voltage transformer steps up the nominal 35-volt main battery voltage to the desired 20-kV output voltage, which is applied to a full-wave bridge rectifier made up of four high-voltage diode assemblies. A filter capacitor re-

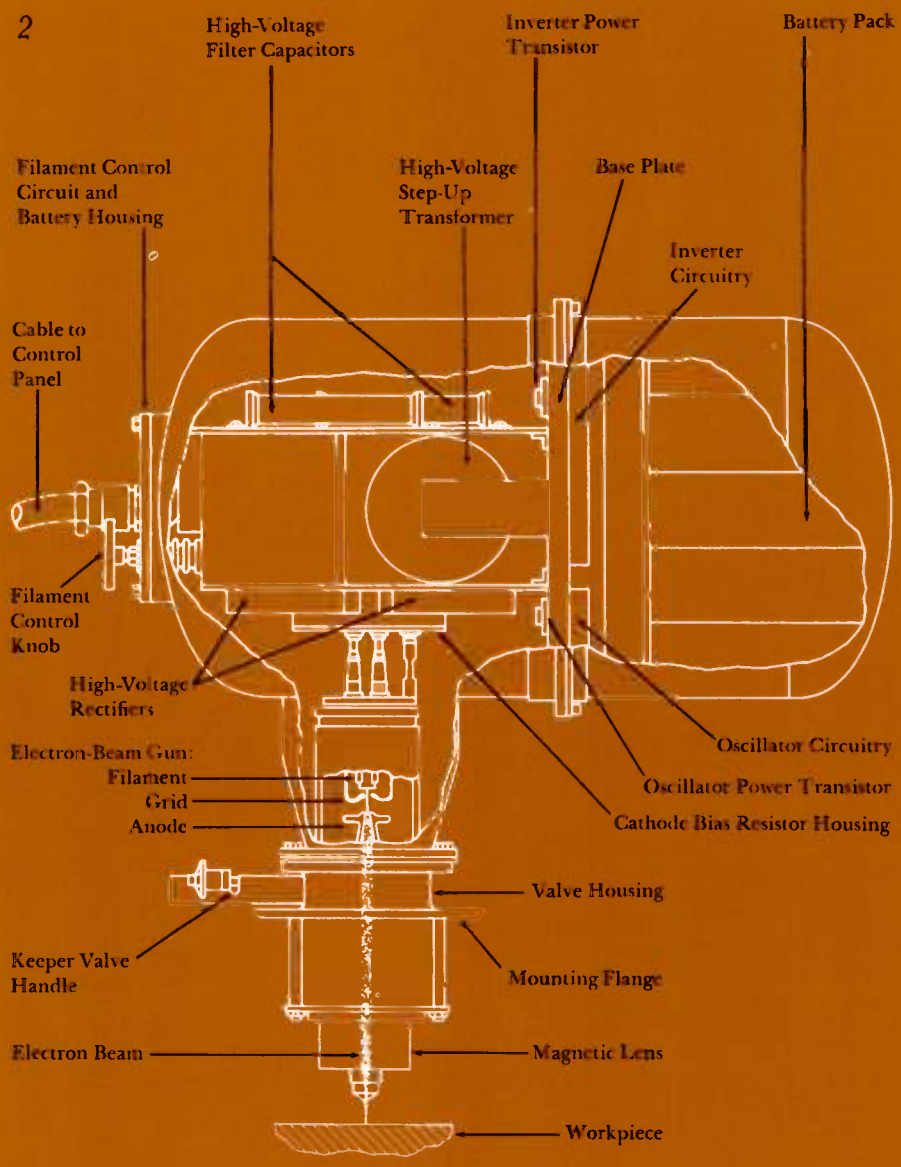

2—Main elements of the laboratory welder are shown in this simplified drawing. It is 21 inches long by 12 inches in diameter, with the lens protruding 10 inches.

duces voltage ripple to less than two percent at full-load current of 100 mA.

A filament battery and control circuit "floats" at the negative 20-kV output of the dc-to-dc converter. The filament battery consists of three silver-zinc cells connected in series to yield 5.5 volts (open circuit) or 4.3 volts under the filament load (nominal 15.5 amperes). The filament control circuit consists of a transistor in series with the filament, a rheostat connected to vary the transistor emitter-base bias, a switch operating from a cam attached to the rheostat shaft, and a jack for charging the filament battery without opening the pressure vessel. The filament can also be operated from an external power source. An insulated extension of the rheostat shaft engages a rotary seal on the pressure vessel end port, enabling an operator to turn the filament on and off and adjust the filament current with a control knob.

The electron-beam gun consists essentially of an anode, grid, and filament. The anode is at case (ground) potential; the filament and grid operate at high negative voltage relative to the anode and are insulated from the anode by the hard-glass envelope of the gun. This glass shell serves also as a barrier between the pressurized sulfur hexafluoride in the converter and the hard vacuum required in the gun.

Grid bias is required for proper focus of the gun but not for current control, which is accomplished by temperature control of the filament. Grid bias is developed by passing the beam current from the converter through a cathode bias resistor to the filament. Typically, a 4000-ohm resistor is used, developing 400 volts negative bias (with respect to the filament) at 100-mA beam current.

A double-acting keeper valve seals the high-voltage chamber of the electron gun to maintain a vacuum in the gun while welding specimens are changed. (When the chamber is again evacuated, the keeper valve must be opened.) Pressure in the high-voltage chamber must be 10^{-4} torr or less for satisfactory operation of the welder.

The gun's magnetic lens refocuses the electron beam at the work—approximately two inches from the center of the lens or about ¾ inch below the end shield. The lens weighs less than one pound, and it requires about 1.3 amperes current from the main battery. A resistor and zener diode preregulator and a miniature constant-current regulator provide constant current to its coil. A meter and a control potentiometer for the coil are provided on the control panel.

With the proper values of grid bias and lens current, 90 percent or more of a 100-mA 20-kV beam passes through an aperture 0.031 inch in diameter. If it is assumed that the cross-sectional beam current distribution is a Gaussian function, then 50 mA of the 2-kV beam would occupy a disc only 0.015 inch in diameter. Weld specimens also attest to the small diameter of the beam (Fig. 3). Beam diameter probably approaches a value limited by lens aberrations.

X rays produced by the electron beam are blocked by the chamber walls if welding is done in a metal vacuum chamber; if a glass bell jar is used, the operators put shielding around the jar or perform the experiments from a remote location. In the orbital experiment, the welding operation will be enclosed in a shielding metal housing with viewing ports of leaded glass.

Flight Model

The most obvious difference between the laboratory welder and the second-generation unit developed from it is the position of the electron-beam gun relative to the converter and battery pack: the right-angle design has been changed to an in-line configuration to produce a more manageable package (Fig. 4). This design is also mechanically sturdier; during launch the unit would be positioned with its long axis parallel to the direction of maximum acceleration.

The second major change is the integral control panel, which contains all the controls and meters necessary for the welding experiments. The astronaut has direct control of the beam current (by varying filament temperature), and he can also vary the magnetic lens current slightly to optimize the beam focus at the work. The high-voltage output of the

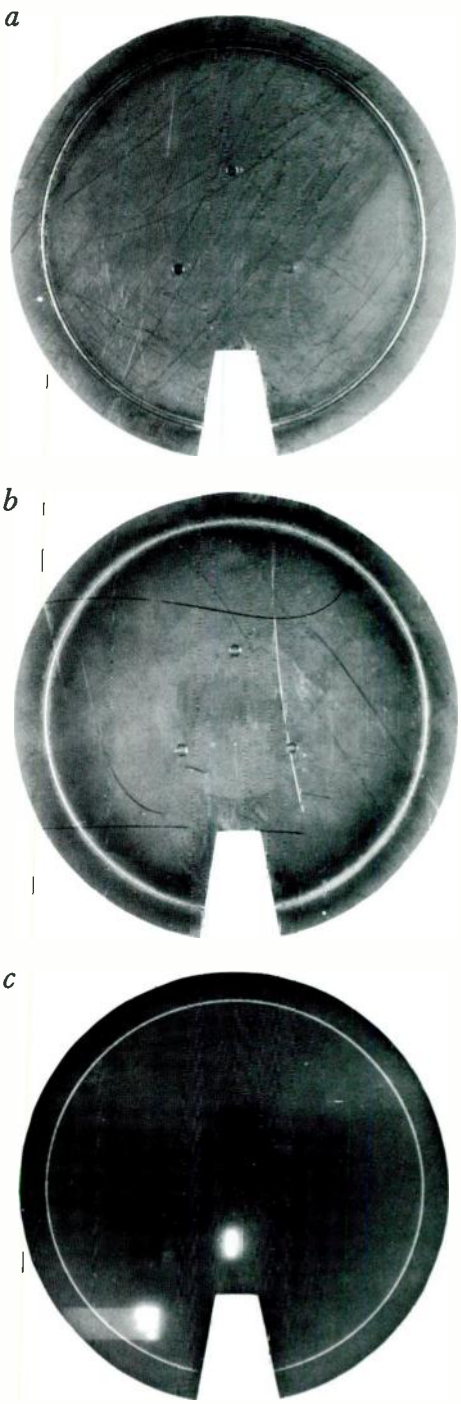

3—Bead-on-plate weld specimen, made with the welder operating completely on battery power, illustrates the high quality of the welds produced. (Front view, *a*; back view, *b*.) It was made in 0.125-inch type 304 stainless steel at 36.8 inches per minute; beam power was 65 mA and 21.5 kV. The radiograph (*c*) reveals no discernable porosity.

4

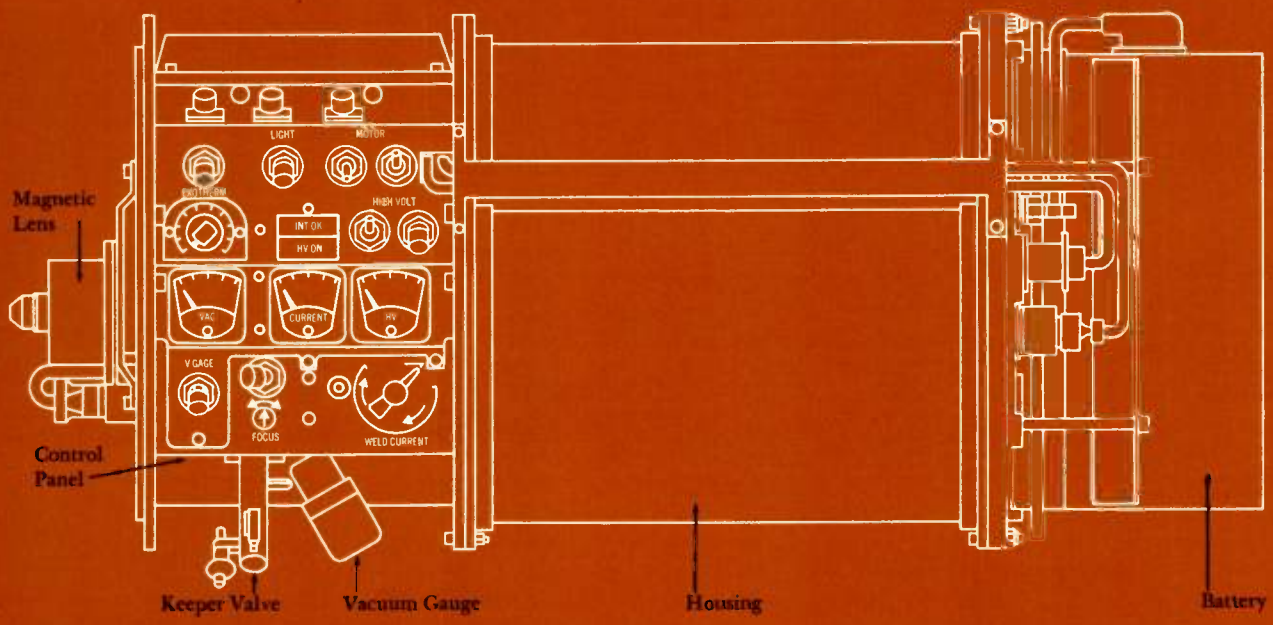

5

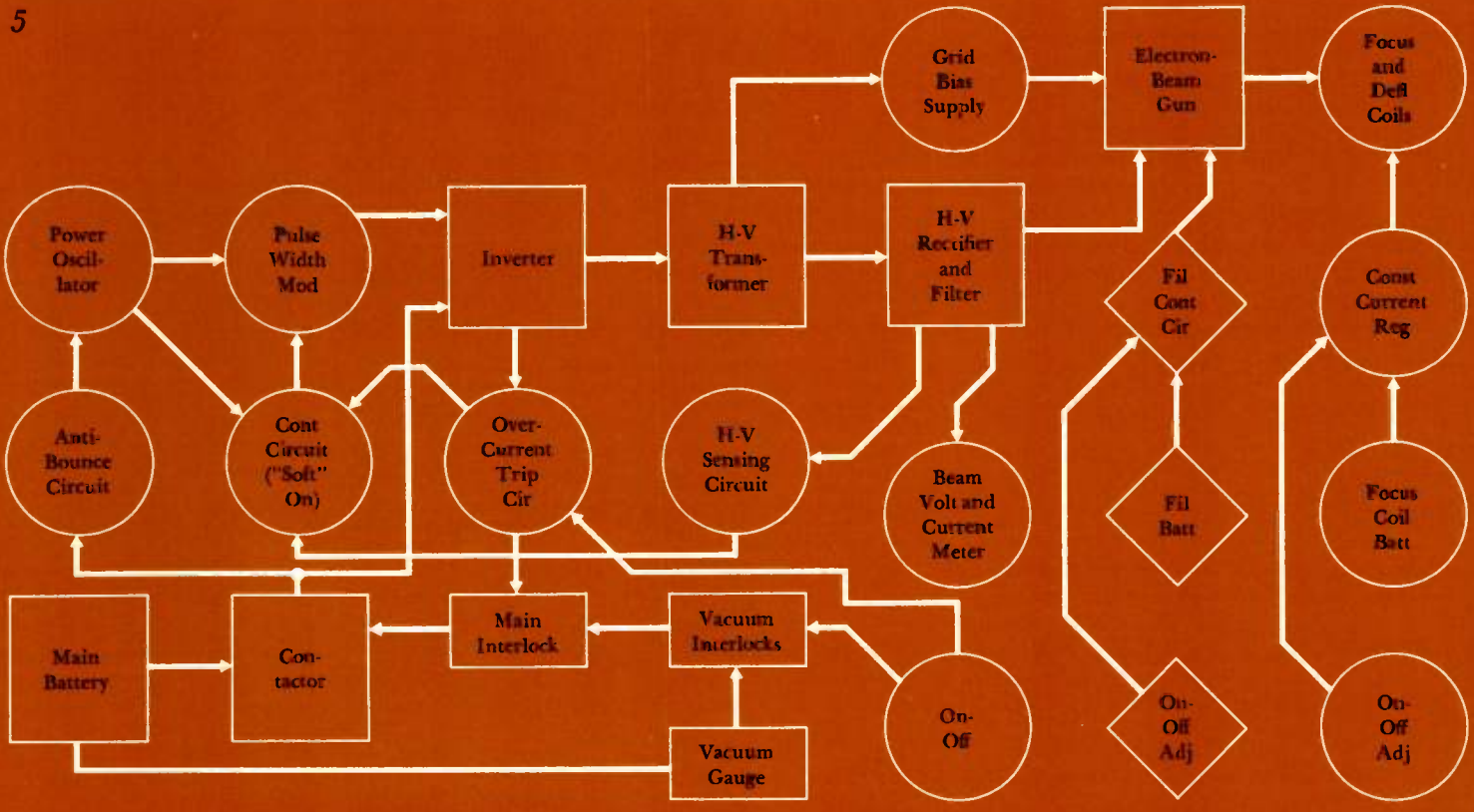

converter is maintained at 20 kV and regulated to better than ±400 volts; no adjustment of this voltage is needed—it is either on or off. Meters monitor the beam voltage and current. Switches are provided for the converter, magnetic lens, specimen drive motor, lights for photography, and an exothermic brazing experiment to be located in the welding chamber.

The electron-beam gun, keeper valve, and magnetic lens were adapted from the laboratory model with only minor changes. The filament control circuit has been modified slightly to obtain increased reliability; the new circuit uses only silicon transistors.

To increase reliability, the original battery pack has been replaced with a Gemini-rated "missile battery" that provides up to 100 amperes at a nominal 28 volts for approximately 10 minutes. Changes in the dc-to-dc converter include use of silicon rather than germanium transistors, individual fusing for each transistor, and addition of voltage regulation and protection circuitry.

The axis of the magnetic lens has been displaced about ½ inch from the axis of the electron-beam gun and two electromagnetic deflection coils added to steer the beam from the latter axis to the former. The purpose is to minimize the possibility that the gun will be damaged by metal fragments created during the welding experiment. The two deflection coils and the lens are all wired in series, and an independent battery and constant-current regulator provide a stable well-regulated current to them. A shunt across the focus coil enables the astronaut to make up to a ±10 percent variation in the lens current with no effect on the current through the deflection coils.

A vacuum gauge is provided for monitoring pressure in the chamber housing the keeper valve. This valve seals against both the high-voltage chamber of the gun and the vacuum chamber where the welding is performed. The gun will be evacuated on earth and the keeper valve closed to seal the gun under high vacuum and thereby minimize the probability of arc-overs. For satisfactory operation, pressure must be 10^{-4} torr or less after opening the keeper valve.

The vacuum gauge is interlocked with the high-voltage circuitry in such a manner that the high voltage cannot be activated unless pressure is satisfactory (Fig. 5). An extraordinary increase in pressure during welding trips off the high voltage. Other functions interlocked with the high voltage include the position of the keeper valve (must be open to close the interlock) and the focus and deflection coil power supply (must be energized to close the interlock).

Beam voltage is regulated by varying the pulse width of the square wave used to drive the inverter. Regulation is required for two reasons: to maintain beam focus on the work with changing battery input voltage and changing beam current; and to simplify the astronaut's control task by enabling him to concentrate his attention on the welding current, quickly setting the current to the desired value without having to adjust the high voltage or the beam focus. The inverter driving signal is generated by a square-wave power oscillator, and the frequency of that oscillator is determined by a low-power relaxation oscillator; thus the frequency is relatively free from change due to battery voltage and temperature variations.

Operation of the converter is initiated by actuating the "on" switch, thus closing the contactor (Fig. 5). The antibounce circuit provides a short time delay before applying the battery voltage to the power oscillator circuitry; the delay allows time for completion of the contact bounce. The power oscillator provides power and synchronization signals for the control circuitry. The control circuitry slowly increases the pulse width of the square wave being supplied from the power oscillator to the inverter through the pulse-width modulator. Thus the inverter initially draws no battery current when the contactor closes, then slowly draws increasing current until approximately 100 amperes (full load) current is reached. Actual battery current is determined by the magnitude of the electron-beam current. The high-voltage sensing circuit samples the nominal 20-kilovolt output and compares it with a reference voltage; the difference between these two voltages is fed back into the pulse-width modulator control circuit so that the 20-kV output is maintained over wide ranges of load impedance and battery voltage.

Since every electron-beam gun is characterized by erratic and unpredictable momentary arc-overs, self-protection of the welder converter circuitry is needed. When an overcurrent condition is detected, the pulse width is rapidly decreased to zero and the main interlock is opened, which, in turn, opens the contactor and removes battery power. Phase-back of the pulse width takes only a few microseconds, while opening the main interlock and contactor requires many milliseconds; thus, the contactor does not have to interrupt the high current of the inverter but only the relatively low current of the power oscillator.

To restart the converter, the astronaut simply actuates the "on" switch. To turn it off, he pushes the "off" switch. This activates the overcurrent trip, which again opens the contactor under a low-current condition.

Conclusion

Electron-beam welding's simplicity of operation, its high efficiency, and its potential applicability to all metals used in space structures make it one of the most promising processes for further development. Design data gathered from the experimental in-orbit welding of various materials should enable development workers to develop assembly and repair welding processes under earth-gravity conditions with confidence of successful performance in space.

4—Later model of the welder was adapted largely from the laboratory model, although the design was altered to locate the electron-beam gun in line with power supply and battery pack. Also, the control panel is integral with the welder.

5—Electrical system includes interlocks for safe operation. In this simplified diagram, square blocks are main power-handling components or circuits, round blocks are control or metering circuits, rectangular blocks are interlock circuits, and diamond-shaped blocks indicate circuitry associated with the gun filament.

The Lunar Television Camera

E. L. Svensson

The Apollo Lunar TV Camera has been designed to operate either in the spacecraft or on the lunar surface with no adjustments except for lens changes.

On the first manned flight to the moon, a small low-power but very sensitive television camera will accompany the Apollo astronauts to send live television pictures back to earth. The camera was developed by the Westinghouse Aerospace Division under contract to NASA's Manned Spacecraft Center in Houston. Hand-held by the astronaut or mounted in the spacecraft, the camera will provide home television viewers with coverage of the Apollo exploration.

In several respects, the camera is unique among the rest of the Apollo electronics equipment. For example, it is one of the few items that must operate under all phases of mission environment —from launch pad to the moon, on the moon's surface, and back to earth. With more than 80 percent of its circuitry in the form of molecular integrated devices, the camera uses fully the most recent developments in solid-state devices. Today's most advanced sensor tube, the SEC camera tube, will enable the camera to operate under the low light level conditions that will be encountered during lunar night.

The main mission of the camera is to provide real-time television pictures of phases of the Apollo mission. A secondary mode of camera operation will provide high-resolution, slow-scan pictures for detailed scientific viewing.

To conserve transmission bandwidth, scanning parameters for the lunar camera are slower than those of standard broadcast television. When received on earth, the pictures will be converted to broadcast television rates for retransmission by commercial stations.

Operational Requirements

Mission environments and compatibility with other equipment place numerous constraints on camera design. As with all space equipment, highly reliable operation is a prime requirement.

Environmental conditions that the camera must withstand are: vibration of 10 to 2000 cycles per second (up to 6 g) and shocks of more than 8 g during Apollo launch and lunar landing; pressure variation from sea level to 10^{-14} mm Hg; temperature extremes on the moon's surface from +250 degrees F during the lunar day to −300 degrees F at night; acoustical noise of 130 dB (above 0.0002 dynes/cm^2). The camera may also be exposed to salt spray, 100 percent oxygen atmosphere, and meteoroid bombardment and particle radiation.

In a spacesuit, an astronaut does not have a great deal of dexterity. Ease of handling, holding, pointing, changing lenses, connecting and disconnecting, storing and carrying without danger of nicking his spacesuit place many constraints on the design of the camera package. Therefore, astronauts need only change lenses and switch scan modes. All other controls within the camera operate automatically. Since the camera will be hand-held, it must be small and lightweight.

Scenes will include views of astronauts moving in the spacecraft and on the lunar surface, the earth or moon from space, the lunar surface, and the LM vehicle on the lunar surface. Light levels for these scenes will vary from partial earthshine on the moon to full sunlight (0.007 to 12,600 foot-lamberts).

A lightweight stowage method is provided to hold the camera and lenses when not in use, within both the command module and the lunar module. It provides easy removal by the astronaut.

Scanning parameters for the camera were selected by NASA to best fulfill the overall mission. Several factors influenced the selection of the scan rates.

Motion rendition must be preserved to avoid breakup in pictures. Ten frames per second provide acceptable motion rendition. Although some motion breakup would occur in normal scenes, an astronaut cannot move quickly in a spacesuit; therefore motion breakup should not occur for the scenes that will be photographed during the Apollo mission.

Ease of scan conversion to 60 frames per second (standard rate) was another factor in determining the frame rate, since submultiples of 60 fps are most easily scan converted. Transmitter bandwidth and power is limited. Since the camera must share bandwidth with voice, biomedical, and other telemetry data, the camera is limited to a 500-kHz bandwidth.

A 320-line scan was chosen to obtain nearly equal horizontal and vertical resolution. Most home television sets reproduce about 300 TV lines from a 525-line scan and provide a pleasing picture. The 10-fps mode will provide a picture of about 250 discernible lines, which is still a satisfactory picture.

For scientific purposes, higher resolution pictures are needed. Since motion rendition is not required for these pictures, a slower scan rate can be used. A scan rate of ⅝ fps with 1280 lines provides a camera in which the sensor becomes the limiting factor in resolution. This rate is also easily obtained from the circuitry that provides the 10-fps, 320-line scan.

SEC Camera Tube

To satisfy the low light level requirements, the SEC (secondary electron conduction) camera tube[1] was chosen. A standard vidicon tube is not sensitive enough and an image orthicon is too large and heavy, and requires too much power. The SEC camera tube is comparable in sensitivity with the image orthicon, but it has the operational simplicity and the lower power requirements of the vidicon.

The SEC camera tube, shown in Fig. 1, consists of three main sections: image section, SEC target assembly, and hybrid gun. The scene is optically imaged on the photocathode, causing electrons to be emitted by the photocathode material (S-20). These electrons are accelerated by the high potential between the photocathode and the SEC target. This target, the unique feature of the SEC camera tube, consists of an aluminum oxide layer, a very thin layer of aluminum, and a low-density KCl film.

E. L. Svensson is a Project Engineer at the Aerospace Division, Westinghouse Defense and Space Center, Baltimore, Maryland.

[1]Goetze, G. W. and Boerio, A. H., "Secondary Electron Conduction for Signal Amplification And Storage In Camera Tubes," IEEE Vol. 52, Sept. 1964.

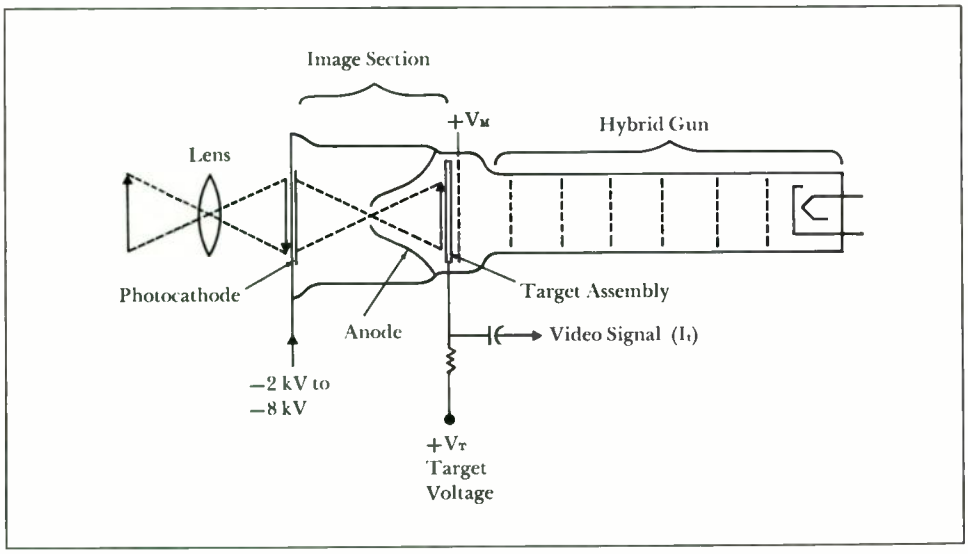

1—The SEC camera tube consists of three main sections—an image section, target assembly, and hybrid gun.

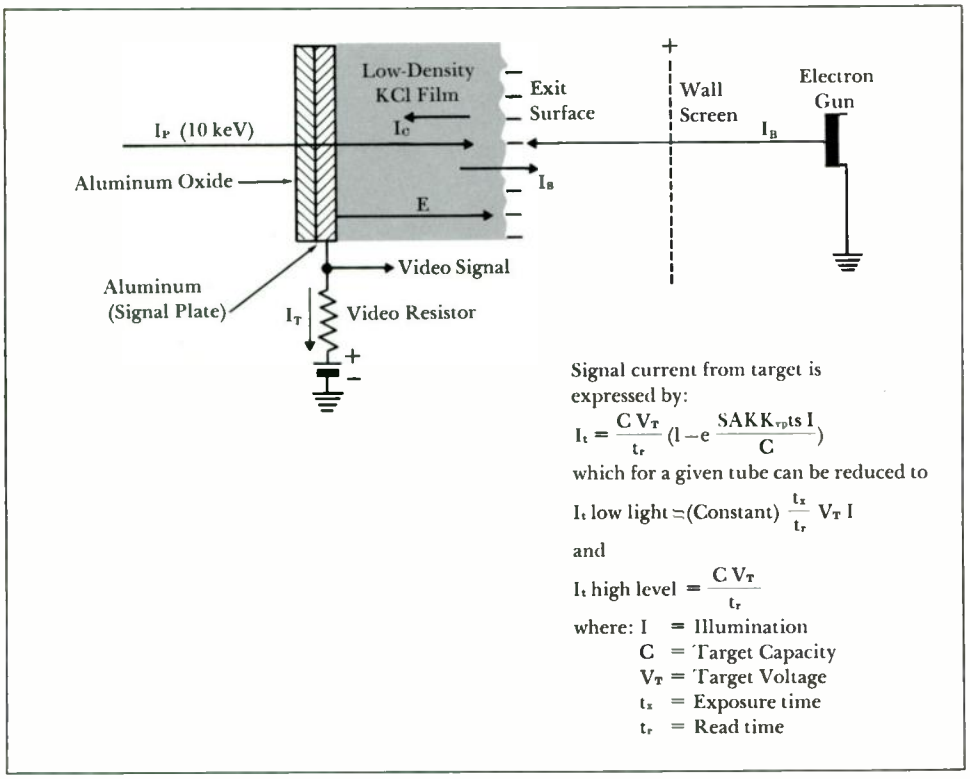

Signal current from target is expressed by:

$$I_t = \frac{C V_T}{t_r}\left(1 - e^{\frac{SAKK_{rp}ts\,I}{C}}\right)$$

which for a given tube can be reduced to

$$I_t \text{ low light} \simeq (\text{Constant})\ \frac{t_x}{t_r}\ V_T\, I$$

and

$$I_t \text{ high level} = \frac{C V_T}{t_r}$$

where: I = Illumination
C = Target Capacity
V_T = Target Voltage
t_x = Exposure time
t_r = Read time

2—Secondary electron conduction (SEC) in low-density film is demonstrated in this diagram. High-energy primary electrons (I_p) release secondary electrons in low-density film. The electric field (E) applied across the film causes a majority of the secondary electrons to be transported through the low-density layer of KCl to produce secondary conduction current, I_c. A fraction of the secondary electrons escape from the exit surface as transmission secondary current, I_s. Gain is the ratio of ($I_s + I_c$) to I_p.

When the accelerated electrons strike the target, they pass through the aluminum layer and strike the KCl film. Secondary electrons released by the KCl film are collected by the signal plate and the wall screen (Fig. 2), leaving a charge pattern in the KCl film. Since the resistance of the film is high, it can hold the charge pattern for long periods until discharged by the reading beam.

The reading beam is supplied by a vidicon-type gun, a hybrid arrangement with electrostatic focus and magnetic deflection (electrostatic focusing permits simple external circuitry and has low power requirements). As the reading beam scans the target, the beam current discharges the KCl film back to cathode potential. This discharging action produces the video signal (I_t).

An important characteristic of the SEC target is that it is almost completely discharged by the beam, leaving negligible signal pattern for the next readout unless recharged by the scene. This eliminates the image smear problems that occur with vidicons and orthicons at low light levels. Of course, smear will occur if the image is moved within a frame period.

Electron gain of the SEC target provides target gains in excess of 100. With an S-20 photocathode, the combined sensitivity of the image section and the SEC target is typically 10,000 μA/lumen. Since target gain is a function of the accelerating potential, target gain is controlled by adjusting the accelerating potential (−2 kV to −8 kV).

Camera Circuitry

Camera circuits can be divided into five major sections, as shown in the block diagram (Fig. 3).

The video output from the SEC camera tube is fed to the video section, which consists of a preamplifier, gain-control element (attenuator), amplifier stages, and a mixing stage. A minimum signal-to-noise (S/N) ratio of 28 dB is required to obtain useful pictures at the ground receiving stations; actually, an even higher S/N is desirable. The low-noise preamplifier is necessary to provide this minimum S/N at the lowest light level (noise equivalent current of the pre-

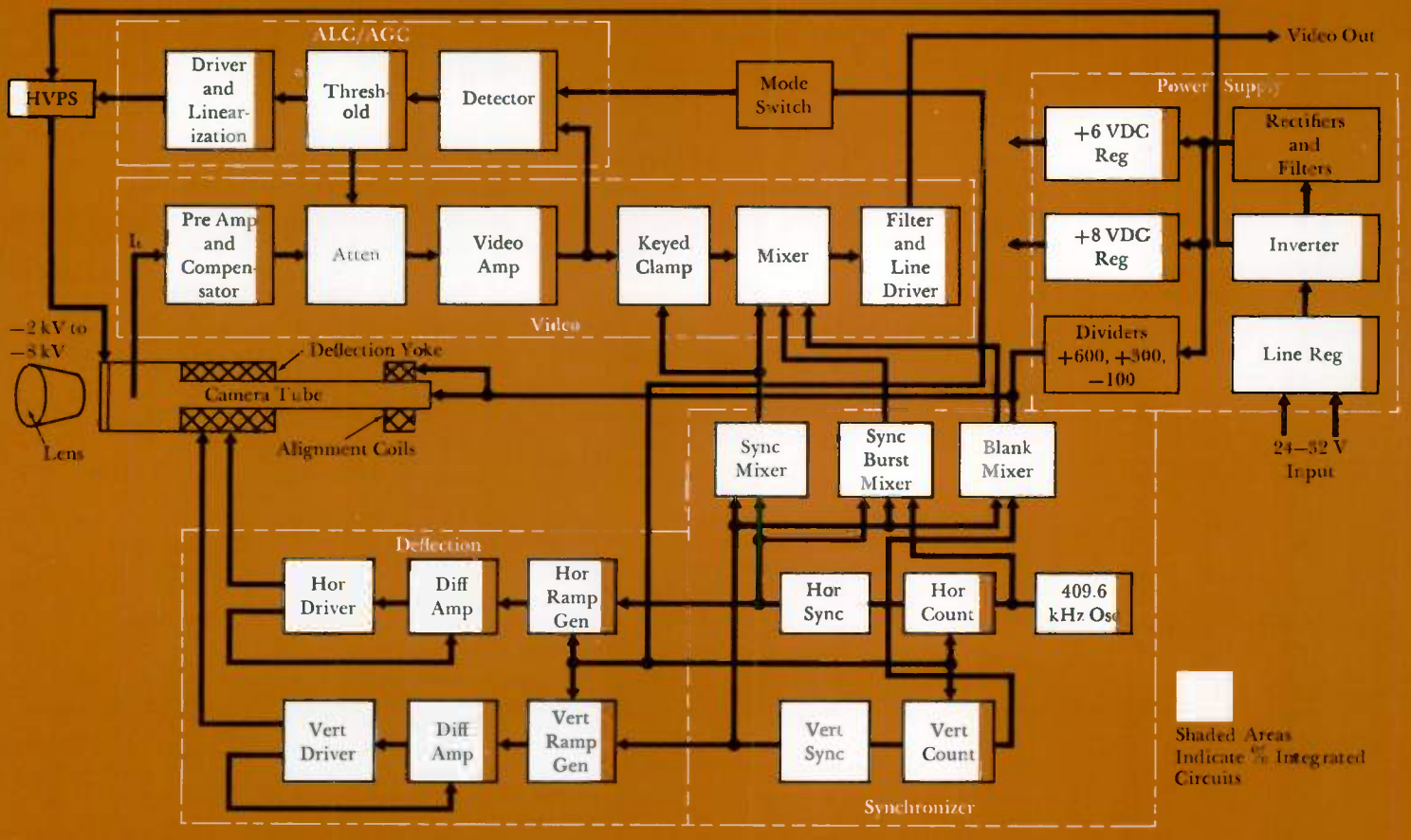

3—Simplified block diagram shows the five major sections of the lunar TV camera.

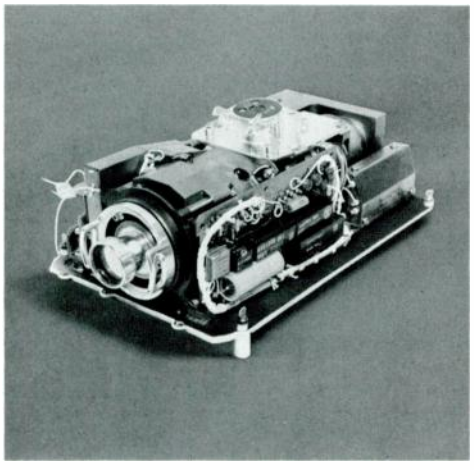

4—(*Top*) A set of four fixed-focus lenses of the quick disconnect type can be easily handled by an astronaut in a spacesuit and provide various fields of view (Table I).

5—(*Lower*) Compact camera package provides for cooling, circuit shielding, electrical insulation, and protection from hostile environments.

amplifier is 2.5×10^{-10} ampere). Overall video-current gain is about 10^6. The mixer stage inserts sync information into the video signal.

The automatic control circuits (ALC/-AGC section) are designed to provide the highest possible signal-to-noise ratio for a given light level, and at the same time maintain a constant signal level out of the camera for a wide range of light inputs. This is accomplished with two gain control paths that operate in sequence.

An automatic gain control (AGC) loop varies video gain at the attenuator to hold a constant output up to the *maximum operating point* (MOP) of the SEC camera tube. At maximum SEC signal current, the saturation level of the SEC target is approached and the picture begins to lose contrast. Therefore, the maximum operating point for the SEC camera tube is chosen just below this level.

When light levels would cause the tube to operate above this maximum operating point, photocathode potential must be reduced to reduce target gain. This is accomplished with the automatic light control (ALC) loop, which controls the high-voltage supply to the photocathode, thus regulating the energy of the electrons striking the camera tube target which in turn regulates target gain. Quality images can be obtained from the camera tube with accelerating potentials over a range of −8 kV to approximately −2 kV, which is the cutoff potential of the image section.

When the camera is operated in the slow-scan mode, the SEC camera tube has a much lower maximum operating point. This is because maximum signal current is proportional to the reciprocal of read time ($1/t_r$, as illustrated in Fig. 2); since slow-scan read time is 16 times longer, maximum signal current is reduced by 16. Therefore, the AGC control loop is switched out for the slow-scan mode and video output is controlled directly by the ALC loop. To provide ease of changing frame rates, all internal switching required is done electronically; a single-pole, double-throw switch, operated by the astronaut, provides the switch signal.

The AGC/ALC control loop arrangement holds video output within a 3-dB variation over a 60-dB range in light level input.

A crystal-controlled oscillator in the synchronizer section provides a stable reference for all timing circuits within the camera. Digital countdown from the crystal frequency (409.6 kHz) generates all timing signals, such as synchronizing signals, blanking, vertical sync serrations, etc.

Linear sweep voltages for deflecting the SEC camera tube beam at the relatively slow scan rates are obtained with closed-loop driving circuits in the deflection section.

Power for the camera is obtained from the spacecraft 28-volt power source, which may vary from 24 to 32 volts. A switched line regulator provides a highly efficient regulation of this input to supply the inverter. All necessary voltages are obtained from the inverter. Two of these voltages—+6 volts and −8 volts used in the sweep, video, and automatic light control circuits—require further regulation because of their varying loads. The −8 kV photocathode supply consists of a separate inverter with a controllable input (for ALC) and a six-stage voltage multiplier, followed by additional filtering to provide extremely low ripple.

The connection to the camera, for bringing power in and the video signal out, must be easily connected or disconnected at any time during the mission. A special connector[2] was designed for the lunar camera since none was available that would operate in a vacuum, salt spray, humid, or explosive atmosphere.

Optical System

Several lenses are required because the anticipated scenes require different fields of view. Furthermore, the light level will vary from 0.007 to 12,600 foot-lamberts for the anticipated scenes. To cover both of these conditions, a set of four fixed-focus lenses were chosen in preference to a zoom lens or a turret system, because either of the latter would have been heavier and less reliable.

[2]Rushing, Frank, "Electrical Connectors for Outer Space Application," *Westinghouse ENGINEER*, March 1966.

Lenses are all quick disconnect type so that they can be handled by an astronaut in a spacesuit. They are listed with field of view and T-number in Table I. (T-number is the combination of f-number and effects of filtering). T-numbers were chosen to set the photocathode illumination within the dynamic range of the camera tube for the various scenes.

Maintaining optical focus for all lenses under all environmental conditions required careful selection of mounting materials and methods. For example, the lenses are mounted directly to the tube assembly rather than to the camera case, which permits closer mounting tolerances to be maintained.

Camera Package

Design of the camera package (Fig. 5) had to accomplish many tasks, such as cooling, shielding circuits from each other, insulating high voltages, preventing corona, and protecting circuitry from hostile environments.

One of the more critical problems was designing the camera to withstand the thermal radiation from both the sun and the 250-degree surface of the moon during the lunar day—and also withstand the cold of the lunar night when the lunar surface drops to −300 degrees F. Limitations of the sensor, optical interfaces, and the electronic components preclude operation at these temperatures.

Passive cooling by radiation was chosen as the most reliable and lightest weight method. Heat generated within the camera circuitry must be conducted to the ground plane (heat radiating surface) since heat transfer by convection cannot occur in vacuum. For example, circuit components are mounted on boards with printed wiring on one side and a ground plane on the other. This ground surface not only serves as a heat conduction path, but also provides necessary shielding.

Thermal balance of the package requires sufficient surface area and a surface finish such that the heat generated by camera circuitry and the incoming thermal radiation can be offset by radiation and reflection from the camera's surface into deep space. Therefore, circuits were designed for minimum power dissipation. Extensive use of integrated circuits helped accomplish this objective. As a result, temperature within the camera will be maintained between 0 and 130 degrees F. All circuits are designed to operate well beyond these temperatures to provide a further safety margin.

High voltages for the sensor plus the varied pressures encountered required special design to prevent insulation breakdown and corona. For example, power supply circuits are molded in epoxy for structural support and for protection against low pressure. The external surface of the power supply is plated and tied to ground to prevent surface charge buildup and corona, and to provide shielding.

A vacuum-tight pressure seal for the camera would have been unreliable and heavy, and therefore was not used. Rather, a seal between the camera covers will keep out humidity, but will allow pressure inside the camera to change slowly.

Table I. Lens Characteristics

Scene	*Light Level (ft-lamberts)*	*Lens Field of View (degrees)*	*Lens T-Number**
Lunar Surface—Night	0.007-1.2	30	1.15
Lunar Surface—Day	20-12,600	30	60
Earth and Moon	20-12,600	7	60
Spacecraft Interior	0.5-300	80	5

**T-number is the combination of f-number and the effects of filtering.*

Table II. Camera Parameters

Power	6.5 watts, 24 to 32 volts dc input
Weight	7.25 lb
Video Bandwidth	2 Hz to 500 kHz
Scene Illumination	0.007 ft-lamberts to 12,000 ft-lamberts
Automatic Control Range	1000 : 1
Scan Parameters	10 frames/sec 320 lines/frame ⅝ frames/sec 1280 lines/frame
Aspect Ratio	4 : 3
Resolution	500 TV lines
Operating Temperature	0° to +130°F
Linearity	2%

Camera Tests

Several cameras identical to the actual Apollo mission cameras were fabricated for environmental testing. Special manufacturing procedures were set up to fabricate the test cameras, and all assembly work was done in a clean room environment.

In addition to vibration, humidity, salt spray, and other environmental tests normally performed on space or airborne equipment, the cameras were tested for operation on a simulated lunar surface. Simulation of the lunar surface for both day and night was done in a large vacuum chamber, with a solar simulator for lunar day tests. After passing the tests for the mission environments, these cameras were then subjected to more stringent environments to determine the amount of safety margin available.

The final tests of the Lunar TV camera will be viewed by millions as they watch, on their home television sets, the exploration of the moon as seen by the Apollo astronauts.

Developing Automatic Load-Shedding Programs with Underfrequency Relays

H. E. Lokay
V. Burtnyk

Automatic load-shedding programs can increase system reliability by preventing total system collapse from emergencies when load exceeds generation.

Frequency deviations are small on today's extensive interconnected utility systems because the stored energy of rotating equipment is large in comparison with normal load variations. Large decreases in frequency can occur only when an affected area separates from the interconnected systems and is left with insufficient generation capacity. Such a separation may result from a major system disturbance that creates large power swings or tie-line flows and causes line relay operations. If insufficient generation to meet load results during these emergencies, an automatic load-shedding program throughout the affected area can prevent total area collapse. A simple but effective automatic load-shedding program can be provided by applying underfrequency relays in substations throughout a load area, preset to drop specific amounts of load for preselected low system frequencies.

Underfrequency relay settings can be developed to drop approximately the minimum load necessary to arrest system frequency decay at a safe operating level. Additional underfrequency relays can also be applied to initiate a safe and orderly system separation or shutdown if the emergency is beyond the capabilities of the load-shedding program.

System Frequency Characteristics

Before considering the design of a load-shedding scheme with underfrequency relays, the behavior of the system during an overload must be understood. The reduction in system frequency with time for different magnitudes of overload is shown in Fig. 1, where overload is defined:

$$\text{Overload } (\%) = \left[\frac{\text{Load} - \text{Sum of Unit Loadings}}{\text{Sum of Unit Loadings}}\right] \times 100.$$

For example, if a plant that had been supplying 20 percent of system load is lost, the overload is $[(1.0-0.8)\div 0.8]\times 100 = 25$ percent.

This value is the initial overload, before any change in input power to the turbines takes place. Actually, for the time span shown in Fig. 1, unit speed-governor action would be initiated by the frequency reduction, and possibly some power increase would be available. However, governor action was omitted because ability to increase input power depends on unit spinning reserve allocation, control sensitivity, and energy system time constants that differ from system to system (and possibly within a single system during different load conditions).

Frequency decay curves are shown in Fig. 1 for three different system inertia constants (H). The overall system H constant is calculated from individual unit H constants, considering only those units that are most likely to be operating for a particular system load condition. For individual thermal units, the inertia constant decreases as unit size increases and as materials are used more efficiently. A typical value for a large modern steam turbine-generator is about 4. Thus, on a system with a substantial part of its generating capacity in large modern units, the system H constant usually is between 4 and 5. If most of the system capacity is in small units, possibly some low-pressure and 1800-rpm units, the system H constant may range from 4 to 7. For an industrial system composed entirely of low-pressure 1800-rpm units, the H constant can be as large as 8. Inertias of rotating loads on the system are generally not included in the calculation because their effect is small and cannot readily be determined.

Another system parameter that affects frequency decay is the load reduction that results from the decrease in system frequency. Although load decrease with frequency varies from one system to another and cannot be accurately determined, its effect is to reduce the rate at which frequency drops and thereby help to stabilize system frequency at some reduced value. A load reduction rate of two percent for each one percent drop in frequency has been listed in the literature as representative for many years. This load reduction rate (arbitrarily called d) was assumed for developing Fig. 1. However, recent work by the IEEE[1] indicates that actually the value may be greater; a range of 1.2 to 7.8 percent load decrease per one percent drop in frequency has been reported.

The effect of the load reduction rate (d) on system frequency decay is illustrated in Fig. 2. These curves are shown for a system overload of 50 percent on a system with an H constant of 4. Similar curves can be calculated for other H constants.[2]

The frequency at which a system stabilizes for overloads of 0 to 100 percent for a range of load reduction rates is shown in Fig. 3. To use these curves, a minimum desired settle-out frequency is selected, and the overload that the system can withstand without having to shed load is then determined. For example, if the minimum desired frequency is 57 hertz, a system with a load reduction rate of 2 can permit an 11 percent overload.

The amount by which a system overload exceeds the limit indicated in Fig. 3 is the amount of load that must be shed. This excess load is shown in Fig. 4 for a system settling at 57 hertz. Similar families of curves can be developed for other values of minimum desired settle-out frequency. The load required to be shed is in percent of total system load in the affected area, and the overload is as defined previously. For example, a loss of 50 percent of the system's generating capacity results in an overload of 100 percent on the remaining units. From Fig. 4, a system with a load reduction rate (d) of two percent per one percent drop in frequency would have to shed about 45 percent of the system load; however, if the system load reduction rate (d) is 6 percent, only about 30 percent of the system load would be required to be shed. The values shown in Fig. 4 are independent of the system H constant because H constant only affects *time* to reach the final settle-out frequency, as shown in Fig. 1.

In the development of a load-shedding program, it is also necessary to know the *rate* of frequency decay for different

H. E. Lokay is Manager, Generation-Rotating Machinery, and V. Burtnyk is a transmission engineer, both in Electric Utility Headquarters Department, Westinghouse Electric Corporation, East Pittsburgh, Pennsylvania.

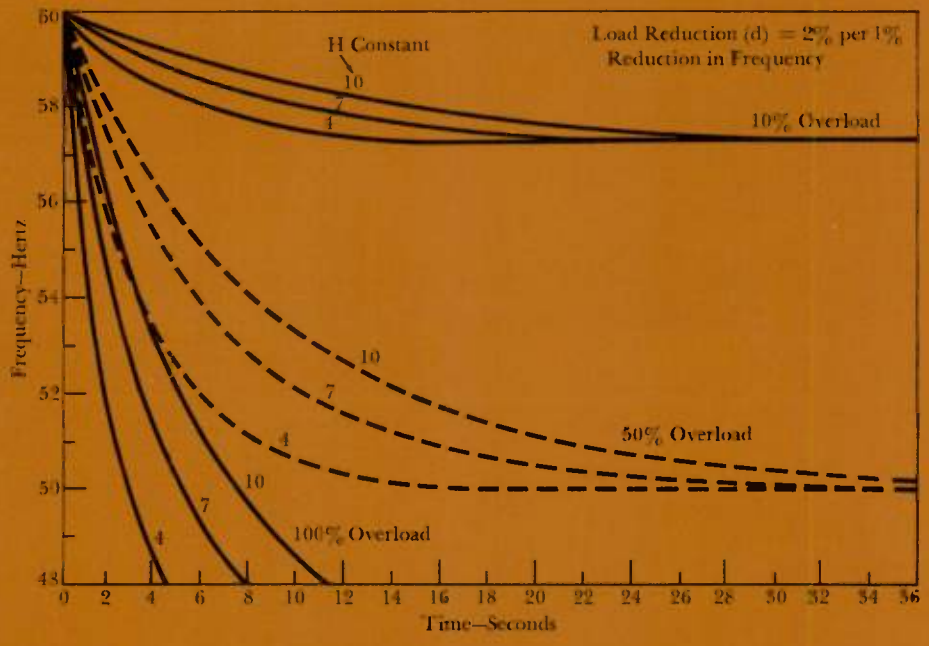

1—Frequency decay due to system overload is a function of the amount of overload, the system inertia constant (*H*), and the load reduction rate (*d*).

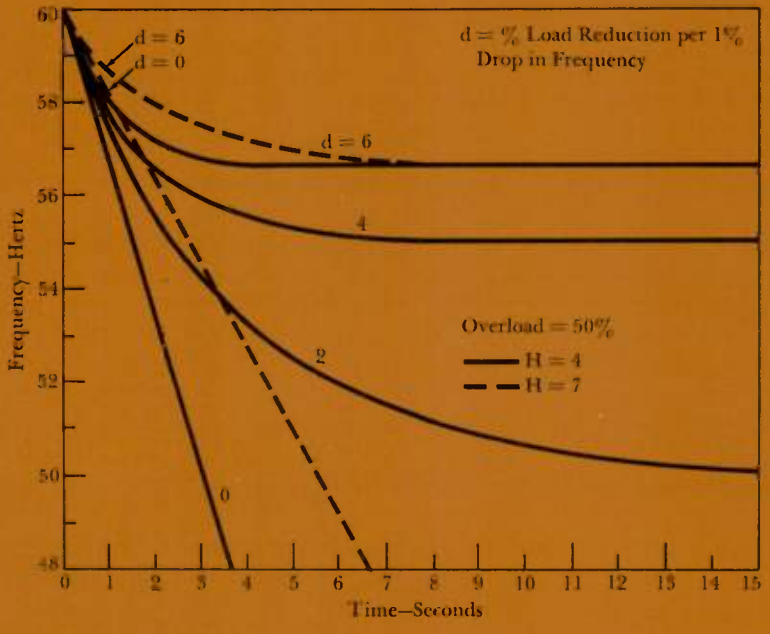

2—The effect of the load reduction rate (*d*) is illustrated for two values of system inertia constant (*H*).

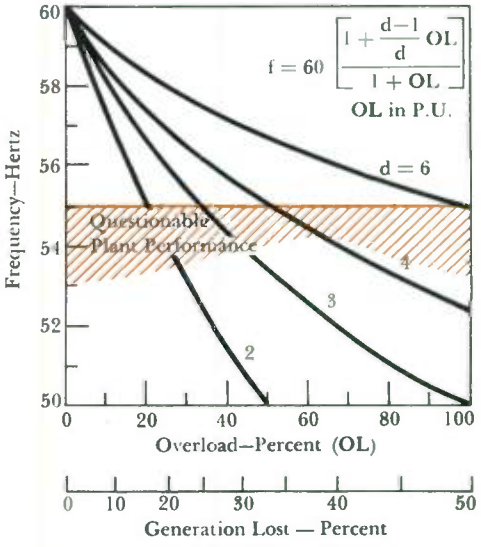

3—Final settle-out frequency is a function of system overload (*OL*) and load reduction rate (*d*), as expressed by the formula.

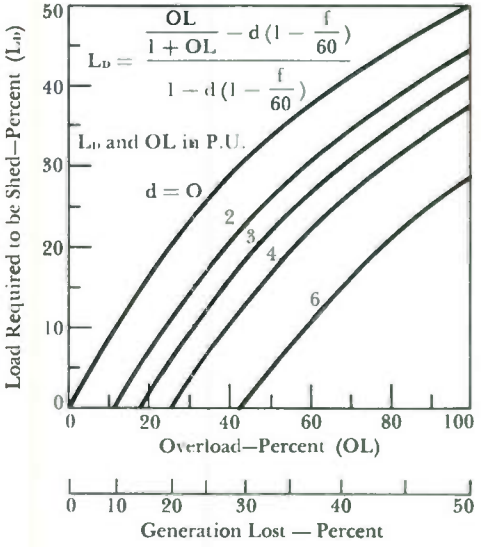

4—Load-shedding requirement (L_D) for a settle-out frequency (*f*) of 57 hertz is a function of overload (*OL*) and load reduction rate (*d*), as expressed by the formula.

magnitudes of generation deficiencies. The rate of decay of system frequency with time is shown in Fig. 5 for overloads of 10, 50, and 100 percent on a system with H constants of 4 and 7 and a 2 percent load reduction rate (d). For a larger load reduction rate, the initial rate of frequency decay would be the same but it would decrease to a small value in a shorter time. For practical magnitudes of area overloads, the rate of frequency decay will probably be less than 3 Hz/sec immediately following the disturbance and system separation. In general, the rate of frequency decay rapidly becomes less than 2 Hz/sec except for very high overload conditions.

Underfrequency Relay Characteristics

Underfrequency relays operate to close their contacts when the system frequency drops below the value preset on the relay. The adjustable range for frequency settings is usually 55 to 59.5 Hz. Relay tripping times after the preset frequency settings are reached are a function of rate of change of frequency. The dynamic trip time characteristic for the Westinghouse KF underfrequency relay is shown in Fig. 6.

Since frequency continues to decay during the deficient generation period, the actual system frequency will have dropped below the relay setting by the time the relay contacts finally close. Therefore, this additional drop in frequency below the relay setting must be determined to coordinate relay settings for successive load-shedding steps. This additional frequency drop must be calculated because the rate of change of frequency decay is not constant due to the load reduction with frequency reduction. Furthermore, circuit breaker opening time and any other additional time delays that occur should be included in the calculations.

A set of curves that illustrate the drop in frequency below relay settings for a range of Type KF relay settings is shown in Fig. 7. These curves were developed[3] from the KF relay tripping time characteristic (Fig. 6) and the rate of frequency decay curves (Fig. 5).

Developing a Load Shedding Program

With the basic system and relay characteristic curves that have been described, a load-shedding program can be designed. The first step in developing the program is to select the percent overload level that the program is to protect, and determine a permissible settle-out frequency for that overload level.

Selecting the maximum overload level is difficult because it is not always possible to predict where an area is going to separate from the interconnected systems, or how much generation will exist in the separated area. However, some insight can be gained from system studies made with digital computer stability programs where line flows versus time following major disturbances can be monitored to determine the more likely areas of system separation. Probable overload levels can then be estimated for the selected areas.

The permissible system frequency decay is primarily determined by limitations or restrictions on steam turbines and power house auxiliaries. In general, continuous steam turbine operation should be restricted to frequencies above 58.5 Hz (60-Hz system base), and operation below 58.5 Hz should be for very limited periods, perhaps 10 minutes or less. However, a load-shedding program can be designed for a lower settle-out frequency than 58.5 Hz *if* the system dispatcher can survey the emergency situation and manually initiate additional load shedding or increase generation (such as peaking unit start-up) in less than 10 minutes. Governor action will also increase input power, if available, within that time. Thus, a load-shedding program based on system frequency settling at 57 Hz when protecting for some maximum overload condition is reasonable. This value is also above the frequency level where plant performance becomes questionable.

And finally, system H constant and load reduction rate (d) must be estimated so that the applicable frequency decay curves can be developed.

To illustrate the development of a load-shedding program, a typical system will be assumed with an H constant of 4 and a load reduction rate (d) of 2 percent. The same procedure would be followed for other system values, but system characteristic data for these values would have to be developed.[3]

Load Steps and Relay Settings

A trial-and-error procedure is required to develop the best combination of number and size of load-shedding steps and the corresponding underfrequency relay settings to protect the desired overload level. An initial combination is selected and checked for relay coordination. Also, the unnecessary load shed is measured when emergency overload conditions are less than the maximum overload used for developing the complete load-shedding program. The results of this analysis will suggest better combinations to be studied.

In general, only a few trials are required to determine the best relay settings for one set of steps and the load magnitude shed per step. Sufficient understanding is generally obtained to minimize the variations tried in number of steps and load shed per step.

The procedure for developing a load-shedding program can be briefly summarized as follows:

1) Determine the total load required to be shed, based on maximum overload for which the load-shedding program is designed and the desired leveling frequency for that overload. For example, from Fig. 4, 44.5 percent load must be shed to protect for a 100 percent overload for a permissible settle-out frequency of 57 Hz when $d=2$.

2) Select the number of load-shedding steps and the amount of load to be shed per step. This selection is arbitrary, but the larger the overload to protect, the greater frequency spread required between successive relay settings. Experience has shown that for most systems, 3 to 5 steps will provide the best correlation between amount of load actually shed and minimum amount required to be shed. Also, the percent of load shed for the first steps should be less than for later steps. Frequently, the number of load-shedding steps and the load shed per step are governed by substation and

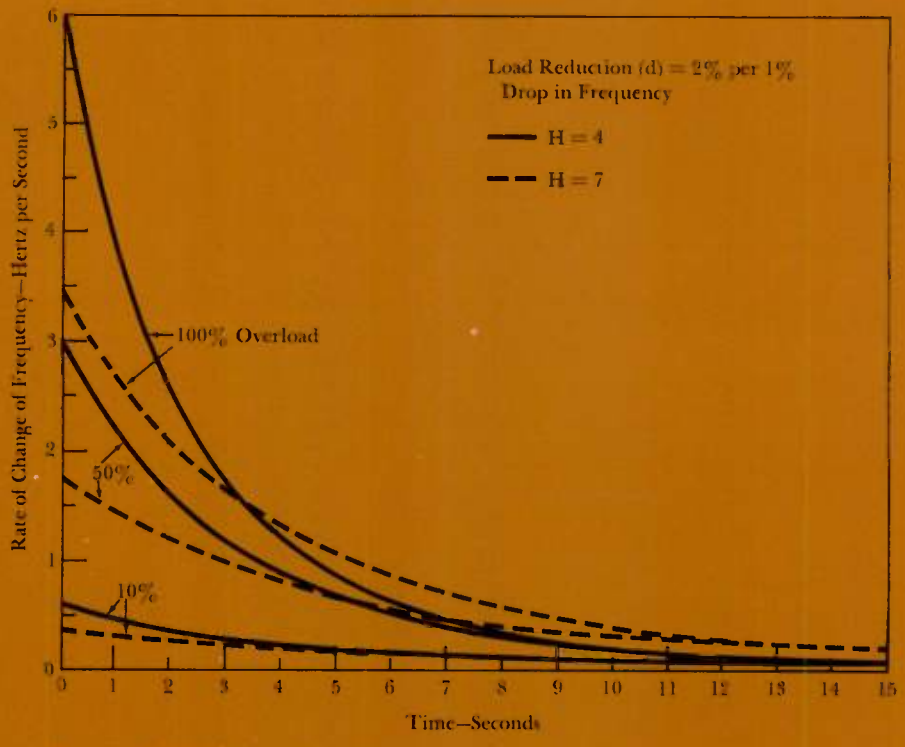

5—Rate of frequency decay is a function of system overload, system inertia constant (H), and load reduction rate (d).

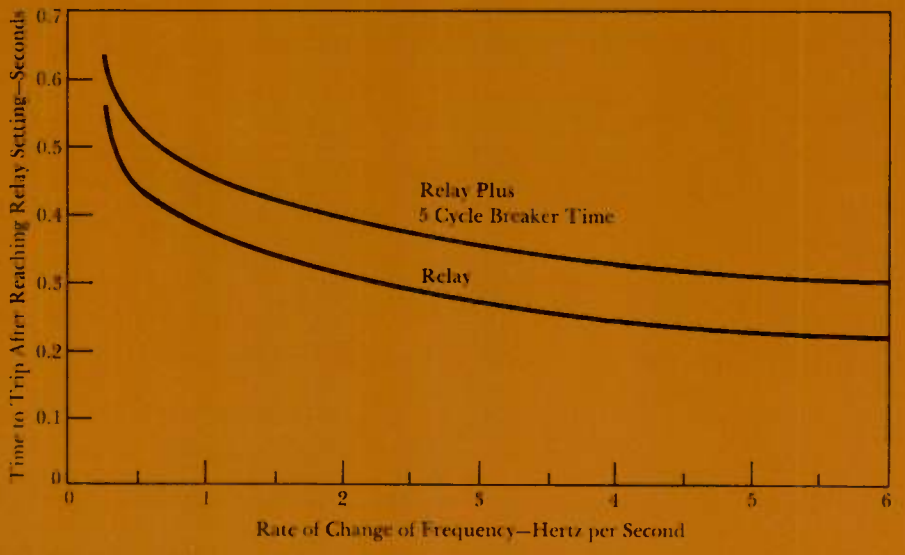

6—Underfrequency relay tripping time characteristic for Westinghouse KF relay with six-cycle time delay.

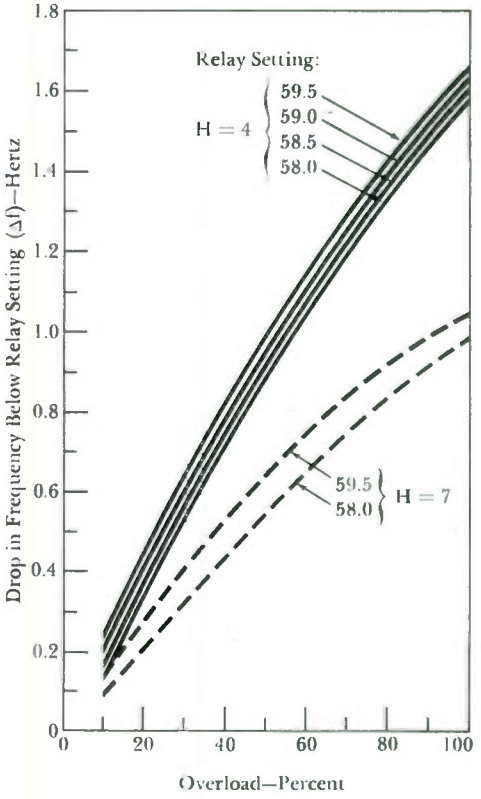

7—Since system frequency drops below the relay setting by the time the circuit breaker trips and sheds load, this additional drop must be considered in coordinating relay setting for succeeding steps. The above curves were developed from the relay-plus-breaker operating time curve shown in Fig. 6 for a system with $d=2$. Similar curves would have to be developed for other relays or breaker tripping times.

8

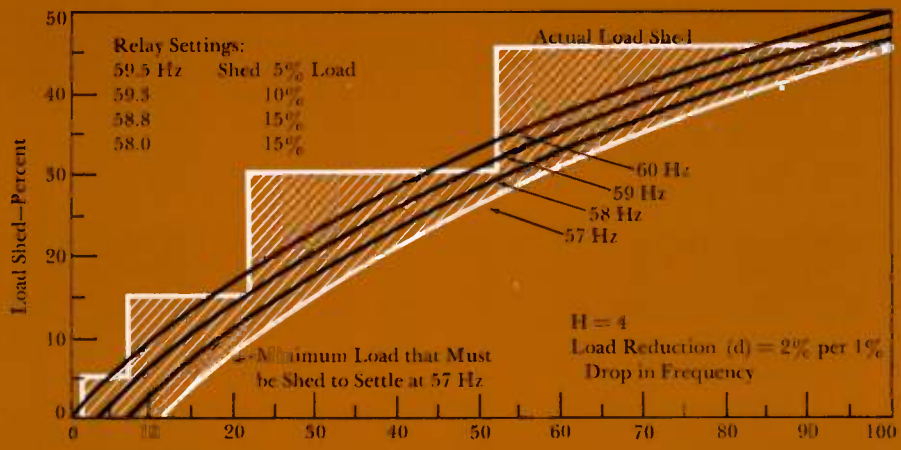

9

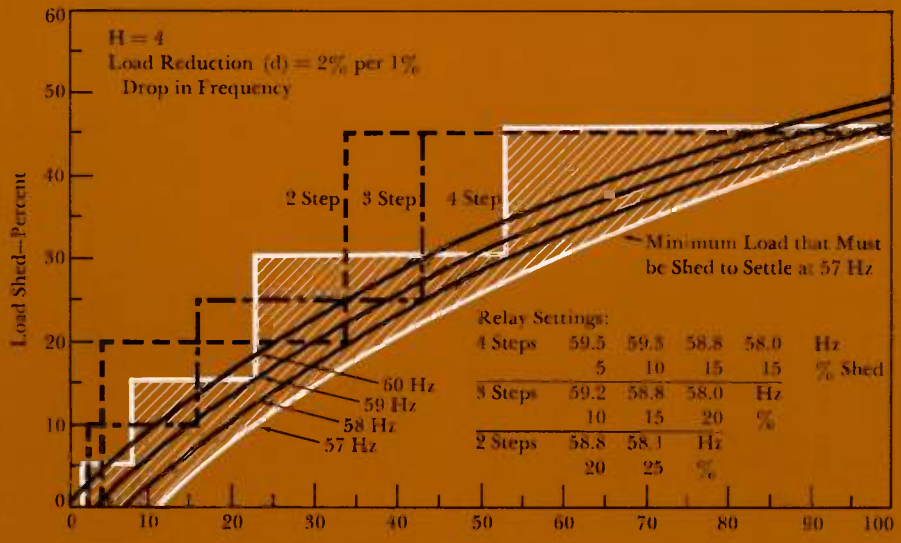

10

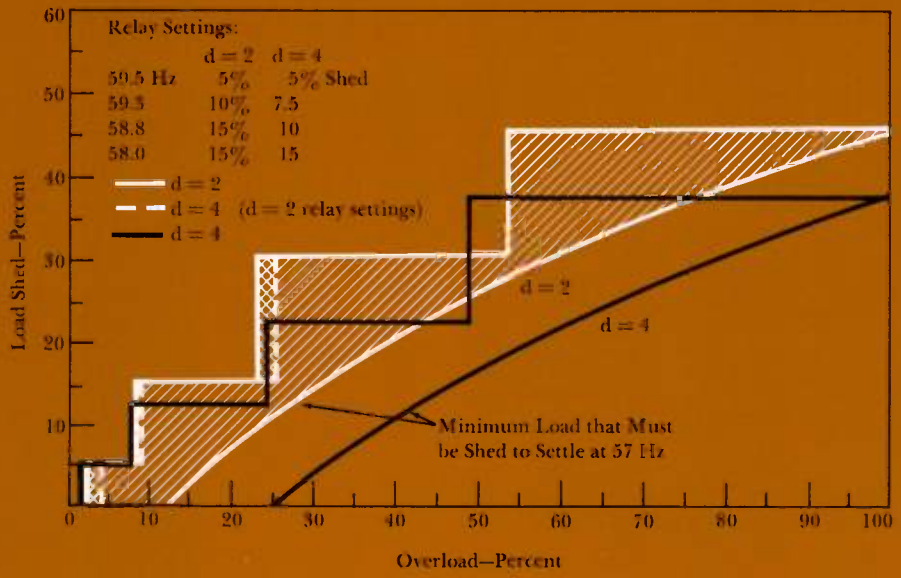

8—Four-step load-shedding program to protect for overloads up to 100 percent (for system with $H=4$, $d=2$ percent).

9—Comparison of 2-, 3-, and 4-step load-shedding programs to protect up to 100 percent overload.

10—Four-step load-shedding programs to protect up to 100-percent overload for systems with load reduction rates of $d=2$ and $d=4$, and performance of a $d=2$ load-shedding program on a system where $d=4$.

feeder arrangements because actual feeders or substations must be assigned to open for each load-shedding step. Also, the assigned feeders must maintain approximately the same percent load being shed regardless of the daily load conditions.

3) Select a trial group of relay frequency settings. A good approach is to divide the frequency spread between the accepted settle-out frequency (57 Hz in Fig. 4) and the highest relay setting available (59.5 Hz) in the same proportion as the load of each shedding step is to the total load shed. For example, four load shedding steps of 5, 10, 15, and 15 percent would have initial trial settings of 59.5, 59.2, 58.6, 57.8 Hz.

4) Check coordination between succeeding relay settings.[3] Coordination of relay settings is required because system frequency will drop below the relay setting before the relay has actually operated. Thus, relay settings must be far enough apart to avoid shedding steps unnecessarily.

5) Check coordination between lowest frequency relay setting (last load-shedding step) and the underfrequency relay settings used for organized system and plant shutdown. These backup underfrequency relays are generally used to protect the system from overloads beyond the load-shedding program. Coordination is required to insure that the additional relays will not operate for overloads within the load-shedding program.

6) Based on the results of steps (3) to (5), select a revised set of relay settings and repeat the calculations. The first trial generally indicates if and how improved settings can be obtained. An indicator that can be useful for improving settings is the area between the appropriate load-shedding step curve and the curve of minimum load that must be shed to settle at 57 Hz (from Fig. 4). This area is shown in Fig. 8. The minimum area that can be obtained while still achieving relay coordination is the combination of relay settings that will drop the minimum excess load for smaller than maximum values of protected overload.

7) Using other combinations of load shed per step and number of steps, repeat steps (2) through (6). The area for each combination can be compared to select an optimum combination for the load-shedding program.

A four-step load-shedding program to protect for a 100-percent overload and to settle at 57 Hz is illustrated in Fig. 8. Minimum load shed curves for settling at 58, 59, and 60 Hz are also included to illustrate the relay frequency settings and to indicate the frequency obtained when the load steps are shed for a specific overload. For example, for a 20-percent initial overload, two load steps would be shed and the frequency would settle at approximately 59.5 Hz. For some overloads, the frequency would actually rise above 60 Hz after the load is shed because more load than necessary is dropped. This is because the program must be developed to protect for some maximum overload since load-shedding blocks are in a few finite steps. For values of smaller than maximum overload, some excess load is shed.

A two- and a three-step load-shedding program for the same conditions as Fig. 8 are illustrated in Fig. 9. The relay settings shown have been optimized for good relay coordination. This comparison illustrates that lower frequency settings are possible with fewer steps, but that greater excess load must be shed for smaller overloads. The increase of area under the three-step and two-step plans, compared with the four-step plan, are 1.12 and 1.32, respectively.

The four-step program as designed for a system with an H constant of 4 and a 2-percent load reduction rate (d) (Fig. 8), but applied to a system where d is actually 4 rather than 2, is shown in Fig. 10. The curves illustrate the unnecessary load that would be shed for this situation and demonstrate the importance of an accurate value of d in developing an effective load-shedding program. By comparison, the desired combination of relay settings and load shed per step when designing for system d of 4 is also shown.

Spinning Reserve and Governor Action

Governor action for increasing unit input power during the emergency has not been considered. Because of the unknowns as to where system separation will occur, available spinning reserve in the affected area, and rate of achieving the spinning reserve, the simplest procedure in developing a load-shedding program is to ignore governor action. Governor action always tends to reduce the overload and therefore the amount of load shed. To include governor action, Figs. 1 and 2 would have to be modified to accommodate the rate of increase in input power. Depending on the type of generation in the affected area, only about 20 percent of the total spinning reserve could be obtained in the first 5 to 10 seconds following a system disturbance.

Conclusion

Characteristics of only one underfrequency relay were illustrated. However, the basic procedure described can be applied for other relay characteristics, or for the same relay with added time delay.

This procedure for developing a load-shedding program using underfrequency relays has given no consideration to physical system restrictions. Also, in selecting the maximum overload that the program is designed to protect, probability values for the occurrence of overloads that are smaller than the maximum overload have not been considered. However, if such probability data is available, it can be a guide in selecting the maximum overload the program should protect. It is best not to design a load-shedding program for an unnecessarily high overload, because the greater this overload, the greater the excess load that is dropped for lower values of overload.

References:

[1]"The Effect of Frequency and Voltage on Power System Load," *IEEE Conference Paper* 31 CP 66-64, presented at the IEEE Winter Power Meeting, New York, New York. (Prepared by IEEE Joint Working Group on Load Characteristics, System Planning and Systems Operations Subcommittee of the IEEE Power System Engineering Committee.)

[2]Fountain, L. L., and Blackburn, J. L., "Application and Test of Frequency Relays for Load Shedding." Paper 54-372, *IEEE Transactions*, Vol 73, Part III, pp. 1660–4.

[3]Lokay, H. E., and Burtnyk, V., "Application of Underfrequency Relays for Automatic Load Shedding," *IEEE Transactions Paper* 31 TP 67-447, IEEE Summer Power meeting, Portland, Oregon, July 9-14, 1967.

Transformer Gas Analysis as a Diagnostic Tool

Harry R. Sheppard

When an oil-filled transformer starts evolving gases, it may be headed for trouble. Regular sampling can detect gas evolution, and then analysis of the gases can indicate their sources and what should be done (if anything) to prevent transformer failure.

The common transformer insulation system of cellulose materials impregnated with oil has been developed through the years to a high state of stability and reliability. Occasionally, however, a transformer evolves various gases (mainly combustible gases) from breakdown of the cellulose, the oil, or both.

Experience has shown that this evolution of gas frequently is not significant—it cannot be related to any transformer malfunction on inspection, and it does not presage transformer failure. At other times, however, the presence of the gases *is* related to malfunction and thus is an indication of transformer trouble.

The presence of these materials in a transformer's gas space is easily detected with instruments developed for that purpose, such as the Westinghouse Combustible Limit Relay. Automatic or routine periodic checking for combustible gas is good preventive maintenance practice. However, gas detection by itself doesn't tell the user what to do about the transformer. He doesn't want to go to the expense of taking it out of service and overhauling it if he doesn't have to, but neither does he want to risk insulation breakdown with consequent loss of the transformer from service and severe damage to it.

Fortunately, studies over a period of years have produced considerable data relating the type and quantity of gas evolved to the state of the transformer's health. Those studies are continuing, with good hope of eventually providing a complete picture of the significance of gas formation. In the meantime, enough has been learned to enable the Power Transformer Division to provide a Gas Composition Analysis service that can indicate when a particular gassing transformer should be examined internally to forestall serious trouble.

Harry R. Sheppard is Manager, Materials and Processes Development, Power Transformer Division, Westinghouse Electric Corporation, Sharon, Pa.

Types and Sources of Gas

Insulation systems are continually being evaluated at the Transformer Divisions by such methods as the functional life test, in which insulation performance in 15-kVA pole-type distribution transformers is observed over a period of time. Moreover, the mechanisms of gas formation from cellulose-and-oil insulation systems are studied specifically. Gas samples resulting from the tests and experiments, and also samples from transformers found to be gassing in the field, are analyzed to determine the types and relative amounts of gas present. Then the types and amounts of gas formed are related to known conditions for producing those gases, and the relationships provide the bases for diagnosis.

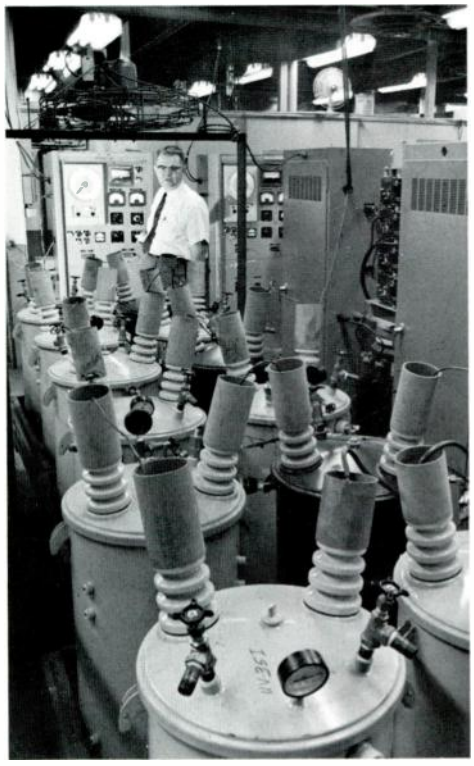

Transformer insulation systems are life-tested in 15-kVA 7200-volt pole-type distribution transformers. Any gas formed is analyzed, and the analyses are correlated with transformer conditions to find relationships that can be used to diagnose transformer ills. Control equipment in the background monitors transformer hot-spot temperatures and periodically cycles the transformers thermally.

The gases found are principally hydrocarbons of low molecular weights, carbon monoxide and dioxide, and hydrogen. They can be formed in different ways.

Since hydrocarbons are usually the principal materials (after nitrogen from the inert-gas blanketing system) found in the gas space of a transformer, the insulating oil is obviously the major source of combustible gas. Experiments have determined the amounts of hydrocarbon gas developed by heating oils. A 0.1-cm³ sample of WEMCO-C oil, for example, evolved 0.00262 cm³ of hydrocarbon gas when exposed at room temperature for five minutes to a vacuum of 1×10^{-6} mmHg (Table I). The sample was then heated to 200 degrees C for 20 minutes and the gas collected and analyzed, and the experiment was repeated at 50-degree C intervals up to 500 degrees C with the results shown in the table. Small quantities of carbon dioxide were detected at about 400 degrees C, but more than 70 percent by volume of the gases evolved were hydrocarbon.

The experiments show that oil heating can produce hydrocarbons and a small quantity of carbon dioxide in a transformer gas space by driving off hydrocarbon constituents of low molecular weight and by some oil pyrolysis (chemical change resulting from heat, which produces mainly methane, ethane, and ethylene). However, no hydrogen resulted even from heating the oil to 500 degrees C. The absence of hydrogen is significant because it shows that hydrogen, which is frequently found when other combustible gases are present, can only result from something other than heat (up to 500 degrees C). That is, any hydrogen found is present because of electrical discharge (arcing or corona), or perhaps because of electrolysis of water or reaction of water with iron.

The paper insulation is the second most important contributor to gaseous decomposition products. Cellulose pyrolysis generally forms large quantities of

water, carbon monoxide, carbon dioxide, and carbonaceous decomposition products in the form of tar or coke. Thus, finding a large amount of the carbon oxides in the gas space of a transformer indicates local overheating of the paper.

Various investigators have found that the principal constituent from the decomposition of oil by electrical discharge is hydrogen: quantities up to 88.8 percent of the total gases have been reported, with small percentages of methane, ethane, acetylene, and other hydrocarbons. Hydrogen also forms in transformers containing water, by reaction of water with iron to produce hydrogen and iron oxide. Another source of gas is electrolysis of water to produce hydrogen and oxygen.

In brief, then, the presence of large quantities of hydrocarbon gases without free hydrogen generally indicates local overheating, with vaporization of oil constituents of low molecular weight and pyrolysis of the oil. Presence of the carbon oxides in large quantity generally means decomposition of cellulose from local overheating in the vicinity of the conductors. Hydrogen in the absence of hydrocarbons usually indicates electrolysis or reaction of water with iron in the transformer, an indication that the transformer should be checked for dryness. However, the presence of hydrogen with appreciable amounts of hydrocarbons might indicate several things, including pyrolysis of oil plus electrical discharge, or pyrolysis of oil plus reaction of water with iron. An analysis that reports the presence of a large amount of hydrogen, carbon oxides, and hydrocarbons is likely to be the most serious because it indicates overheating of the cellulose insulation, overheating of the oil, and possibly electrical discharge.

Gas Analysis Service

The Gas Composition Analysis service provided by the Power Transformer Division utilizes the known correlations summarized above to assess the health of a gassing transformer. The user employs a kit that includes valved sample bottles and instructions on how to purge a bottle, fill it with a sample from the transformer gas space, and send it for analysis. (The Inertaire blanketing system used in most Westinghouse power transformers facilitates sampling because the slight positive pressure of the nitrogen gas makes it easy to fill the sample bottle.) Gas analyses are made with a mass spectrometer at the Westinghouse Research Laboratories, supplemented by a gas chromatograph at the Power Transformer Division.

The following examples of actual analyses indicate the usefulness of the service.

One power transformer had been generating a great deal of gas for several months. The oil was sampled and found to be in satisfactory condition. A sample of gas was removed and analyzed, with the results presented in Table II, *A*. The gas analysis indicated a slow breakdown of oil not associated with cellulose insulation breakdown, as the carbon dioxide content was low. Breakdowns of this nature may be caused by heating and electrical discharge resulting from poor connections, improperly insulated core bolts, or other small discharges to ground. The source can often be found by internal inspection for signs of overheated connections, smoke tracks, or carbon deposits. (It may first be desirable, though, to monitor the combustible gas level with a meter at monthly intervals to determine if the minor fault is continuing to produce gas.) This transformer was inspected internally. All components were found to be satisfactory except that the identification plate on the core had burned ends and carbon deposits surrounding it. The plate had been secured to the core by driving pins in between the core iron, and the pins had been inserted in such a manner that the plate shorted across the laminations. Proper installation required that the pins be driven parallel along the same lamination; replacing them in that manner corrected the problem.

An autotransformer was found to have about 20 percent of combustible gas in the gas space. It was opened for internal inspection, but there was no evidence of the source of gas: leads, terminal boards, tap changers, and so on were all clean and in good operating condition. Resistances of the various winding sections, and ratios of all phases, were satisfactory. However, the characteristic odor of transformer oil in which an arc has occurred was detected, so the transformer was refilled with oil and voltage was again applied. Combustible gas content was measured and found to be 4.5 percent, and in the following days it returned to 20 percent. The gas was analyzed (Table II, *B*). The large amount of hydrogen

*Table I. Volatile Hydrocarbons in WEMCO-C Oil**

Temperature (°C)	Gas Volume (cm^3)			Gas Composition (mol %)		
	Hydrocarbon	Water	Carbon Dioxide	Hydrocarbon	Water	Carbon Dioxide
25	0.00262	....	....	99.99	..	..
200	0.00644	0.00215	....	75.0	25.0	..
250	0.00500	0.00215	....	70.0	30.0	..
300	0.00454	0.00172	....	72.5	27.5	..
350	0.00265	0.00155	....	63.2	36.8	..
400	0.00363	0.0091	0.00027	75.4	19.0	5.6
450	0.00429	0.00091	0.00017	79.8	17.0	3.2
500	0.00639	....	0.00034	94.9	5.1	..
Total	0.03356	0.00939	0.00078			

**Determined with mass spectrometer. Oil sample size 0.1 cm^3.*

and hydrocarbon gases indicated the presence of a hot spot, probably accompanied by electrical discharge, and there was a slight indication of insulation decomposition. Dismantling revealed that a defective static plate had permitted a fault across the static-plate gap, forming a carbon path.

The results of another autotransformer analysis are shown in Table II, *C*. The gas contained a significant amount of carbon dioxide, indicating burning of some cellulose insulation. In addition, the presence of some hydrogen indicated a small amount of electrical discharge. Since the presence of other combustible gases indicated decomposition of oil, a winding fault was suspected. Internal examination revealed a short in a transposition that produced a hot spot in the winding.

Gas samples from a power transformer were analyzed over a period of six months; a typical analysis is shown in Table II, *D*. The large amount of hydrogen and oxygen, with the absence of hydrocarbon gases, indicated the presence of water but no oil decomposition. Lack of appreciable amounts of carbon dioxide and carbon monoxide indicated that the cellulose insulation was not being burned. It was concluded that the combustible gas was caused by water in the transformer reacting with iron in the presence of air. The transformer was carefully inspected, and a large amount of water was found. No oil or insulation decomposition, nor electrical trouble of any sort, was found.

Data from another autotransformer is shown in Table II, *E*. The presence of a small amount of carbon dioxide and of hydrogen and hydrocarbon gases indicated decomposition of some cellulose insulation and oil. The presence of an appreciable amount of hydrogen also indicated electrical discharge. A circulating pump motor was found to be burned out. The motor was replaced and the oil thoroughly vacuum treated, and succeeding gas checks showed essentially no combustibles.

The initial analysis of gas from yet another autotransformer showed 0.83 percent combustible gas with some carbon dioxide (Table II, *F*), indicating breakdown of oil accompanied by breakdown of some cellulose. Gas continued to accumulate, and six months after the first analysis the unit was purged with nitrogen. After another six-month period, the unit was taken out of service. Gas analysis at that time showed 3.82 percent combustibles, mostly hydrogen and methane, indicating continued oil breakdown. Carbon dioxide content was less than in the first analysis, indicating slowing of the cellulose breakdown. Inspection revealed a large amount of carbon soot from oil breakdown, which obviously had occurred over a long period of time. The carbon was distributed over all three phases. The breakdown was found to be caused by a turn-to-turn failure; the insulation had burned through initially in a spot about one inch in diameter, but the failure area had not expanded.

Conclusion

Thus, the insights gained in laboratory investigations are supported by examination of specific units. While relatively few transformers produce gas, and opportunities to obtain case-history data are therefore limited, nevertheless the data that have been obtained have been extremely useful in understanding the causes of gas generation. This understanding is being used for diagnosing specific troubles. Equally important, it can also dispel a user's anxiety by showing that his transformer is not in danger.

Table II. Gas Composition Analyses for Six Transformers

Gas Component	*A*	*B*	*C*	*D*	*E*	*F*	
	Composition (wt %)	*Composition (wt %)*	*Composition (wt %)*	*Composition (wt %)*	*Composition (wt %)*	*Composition (wt %) Analysis 1*	*Analysis 2*
Nitrogen	98.56	94.91	95.99	84.25	..	98.04	95.85
Oxygen	0.47	0.08	1.05	11.68	..	0.60	..
Argon	0.03		0.11	0.56	0.24		0.05
Carbon Dioxide	0.05	0.11	0.45	0.05	0.37	0.53	0.28
Hydrogen	0.25	3.00	0.56	3.46	1.19	0.54	2.08
Carbon Monoxide	..	Trace	..	..	..	0.04	..
Methane	0.32	1.28	0.61	..	0.96	0.25	1.09
Ethane	0.20	0.10	0.11	..	..	..	0.65
Ethylene	..	0.51	0.32	..	0.31	..	..
Acetylene	..	..	0.64	..	..	..	..
Propane	..	..	..	..	..	..	..
Propylene	..	..	0.16	..	0.07	..	..
C_4-C_5 Hydrocarbons	..	..	..	..	..	..	..
Higher Hydrocarbons	0.12	..	..	..	..	..	..

Pulmonary Simulator Developed for Human Breathing Studies

A machine that breathes is taking the place of human volunteers for testing and calibrating medical devices and life-support systems. Called a pulmonary simulator, it inhales ambient air and exhales warm moist air (laden with carbon dioxide) at the same rate as a man (or a woman, or a party, for that matter).

The machine can be controlled to produce any normal or abnormal breathing pattern and can keep at it day and night. Because of that ability to set a known and unvarying pattern, research investigators don't have to keep checking its breath with other instruments or making assumptions about it as they do when working with people. By increasing the volume of gases exchanged in each breath, the machine can be made to fill in for as many as 10 persons. Thus, it can simulate the crew of a spacecraft or undersea craft whose air system is being tested. Simulating just one person, it is used for such purposes as evaluating a respiratory gauge that measures a hospital patient's breath to determine his oxygen consumption.

The machine was developed and is being used at the Westinghouse Research Laboratories. Precise controls were required to simulate the subtleties of breathing; in exhalation, for example, the temperature and concentrations of water vapor and carbon dioxide increase as the air comes up from deeper parts of the lungs, while oxygen concentration decreases and the velocity of the breath climbs to a peak before trailing off.

Pulmonary simulator takes the place of one or more human subjects for such purposes as testing and calibrating medical devices and life-support systems. An oxygen gauge is being connected here.

Small Computer Used to Estimate Cost Factors in Electric Home Heating

A small portable analog computer is helping remove the guesswork from estimating heat loss from a new or older home when the homeowner is considering electric heating. The computer not only analyzes heat loss in a few minutes but also estimates annual electric heating cost and shows how much money the homeowner can save by adding insulation in various places and storm windows and doors.

A compact analog computer provides fast and realistic estimates of heat loss from a house, the contributions of various parts of the structure to heat loss, and the cost of electric heating for that house. The computer can also indicate the effects of changes in insulation on heat loss and heating cost.

The computer is built into an attache case and operated on 115-volt power. It has four rows of knobs for putting in information about areas and insulation for windows and doors, walls, ceilings, and floors. The first knob of each row is set to the correct area for each building section. The second knob of each row is then set to indicate the value of the insulation used (except for the window and door knob, which is set for either single or double glass). An additional knob is provided for basement heat loss; it has settings for full or partial heating and for the amount of wall area that is above grade. There is also another knob for floors, set to indicate whether the floor is over a ventilated crawl space, unventilated crawl space, basement, or slab.

In addition to the information put in with the knobs, each circuit has built-in impedance to account for the heat-loss factors of average residential construction. Also, the computer is preset for local temperature conditions and power cost.

When all the information is dialed in and the selector switch is in the *KW* position, an indicator needle immediately shows total heat loss in kilowatts. The operator then moves the selector switch to the *COST* position, and the needle shows estimated annual heating cost. The operator also can show the effects of changes of insulation in the four areas by adjusting the appropriate knobs.

The Electrocomp computers are made by Beckman Instruments, Inc. They are being made available to electrical contractors and electric utilities by regional offices of Bryant Electric Company, a division of Westinghouse. Since operation of the computers is fast and simple, the offices can take information by telephone and provide the answers immediately.

New Cobalt-Base Magnetic Alloy Remains Useful at High Temperature

A cobalt-base alloy devised recently retains excellent magnetic properties, and also high yield strength and creep resistance, at temperatures up to 700 degrees C. The alloy was developed as part of a program for providing high-tempera-

ture materials for space vehicles, although its properties probably qualify it for other uses as well.

The specific space application foreseen is in the rotating generators expected to be needed as space vehicles increase in size and complexity and thus in power requirements. Severe size and weight limitations will make it necessary to operate the generators at high speeds and temperatures. Conventional wound rotors seem to be ruled out by those conditions, since the severe stress and high temperature would cause the windings to shift and unbalance the rotor. Consequently, a generator type with a solid rotor appears necessary. The rotor material must remain magnetic at high temperature and be strong enough to resist permanent deformation ("creep"); if the rotor were to lose its magnetic properties, or creep enough to fill the gap between it and the stator, the mission would fail.

The new alloy consists of cobalt, nickel, iron, aluminum, and tantalum with small amounts of zirconium and boron. A precipitation-hardening heat treatment is applied to bring about the most favorable microstructure.

At 650 degrees C, the new alloy has a yield strength of 86,000 lbf/in² (at 0.2 percent deformation) and a total creep of 0.2 percent in 10,000 hours under a 50,000-lbf/in² load. At that temperature, a dc magnetizing field of 100 oersteds produces a magnetic flux density of 10.3 kilogauss. At 700 degrees C, the alloy can support a load of 25,000 lbf/in² for 10,000 hours with 0.2 percent creep while retaining excellent magnetic properties.

The alloy was developed by the Westinghouse Research Laboratories for the Aerospace Electrical Division in a program with the National Aeronautics and Space Administration to improve high-temperature electrical materials.

Uninterruptible Power Supply Serves Defense Communications

A 250-kW uninterruptible power supply is being installed for a defense communications network in the Pentagon. It is a static inverter system capable of maintaining a continuous flow of electric power if normal commercial power is interrupted momentarily, or for longer periods up to 15 minutes (during which time standby generators would be started and would pick up the load).

In a commercial power outage, the stored energy from 48,000 pounds of lead-calcium storage batteries would supply dc power, which would be changed to ac power by the inverter system. The load is connected to the inverter system at all times; when normal power is available, the batteries are continuously being charged so that they are always ready.

To insure continuity of service, three 156-kVA units are operated in parallel. Any two units are capable of supplying the load. The units occupy a space 22½ feet long, 5 feet deep, and about 8 feet high. They were built by the Westinghouse General Control Division.

Packing More Inverter Capacity into Smaller Packages

Spacecraft power systems are continually increasing in capacity as vehicles become larger and missions more complex, and that growth increases the size of the static inverters presently used to supply ac loads. Consequently, new approaches are necessary to decrease size-to-power ratio.

Since much of the size and weight of a conventional inverter is in the filter needed to convert the basic square-wave power output to a sine-wave output, reducing the filter size by a large amount would be an effective way to reduce the overall inverter size. A new circuit concept called staggered-phase carrier cancellation does just that. It promises to reduce size and weight of sine-wave inverters for spacecraft and aircraft at least 50 percent, depending on power level, and achieve an efficiency of 90 percent or more. Besides inverters, another possible application of the concept is in audio amplifiers of higher power output than is now feasible —several kilowatts.

The conventional (and simplest) approach to sine-wave inversion is to use solid-state switching elements in a circuit that breaks up the dc input and rearranges it as a square-wave ac output voltage, and then filter out all harmonics of the fundamental to leave a pure sine wave. Although some of the latest static inverters produce a stepped wave to approximate a sine-wave output, much filtering still is required.

The new circuit concept worked out at the Westinghouse Research Laboratories takes advantage of the ability of recently developed transistors to switch power efficiently at much higher frequencies than those used in conventional inverters. Use of higher frequency synthesizes the output waveform in far smaller pieces, producing a much closer approximation to a sine wave than the square waves produced by conventional inverters. There are no harmonics of the fundamental wave to filter out, and the carrier harmonics that do have to be filtered out are so high that small filters suffice. (Filters decrease in size as frequency increases.) Besides greatly reducing system size and weight, reduced filter size also reduces output impedance and phase shift and thereby simplifies inverter paralleling.

The circuit employs pulse-width modulation (Fig. 1). Each of the waveforms in Fig. 1a represents a train of square waves modulated by the signal shown in Fig. 1b. If such a pulse-width-modulated (PWM) waveform were passed through a low-pass filter with a cutoff frequency slightly lower than the carrier frequency, the continuously varying asymmetrical square wave would reduce to a sine wave. The main advantage of sine-wave synthesis in this manner is that the filter need only reject the carrier and its harmonics, rather than harmonics of the desired output frequency; by making carrier frequency as high as possible with respect to the desired output frequency, filter size is made much smaller than it can be in the conventional approach.

The carrier frequency is about 10 kHz. It cannot be made higher in a simple PWM circuit because of the limited switching speed of the transistors.

However, the new circuit concept *multiplies* that already high carrier frequency *by a factor of four*, thereby reducing still more the size and weight of the output

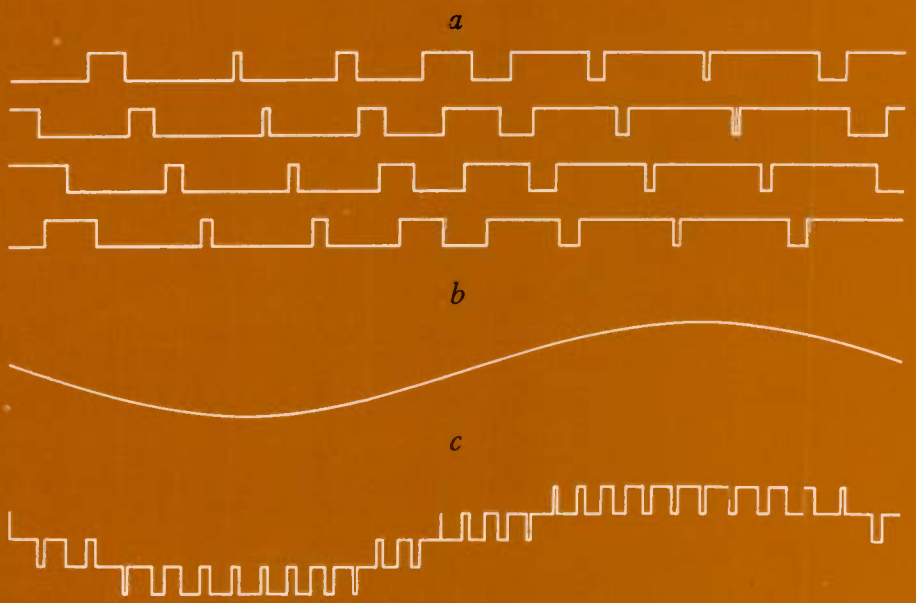

1—Sine-wave construction by staggered-phase carrier cancellation begins with pulse-width modulation of high-frequency square waves, as in *a*, with a power-frequency sine-wave signal *(b)*. By producing the pulse-width-modulated (PWM) waves out of phase, as shown in *a*, and combining them, the carrier waves are cancelled while the modulations of the four waves are added *(c)*. The results are great reduction of filter requirements and strengthening of the power output of the inverter.

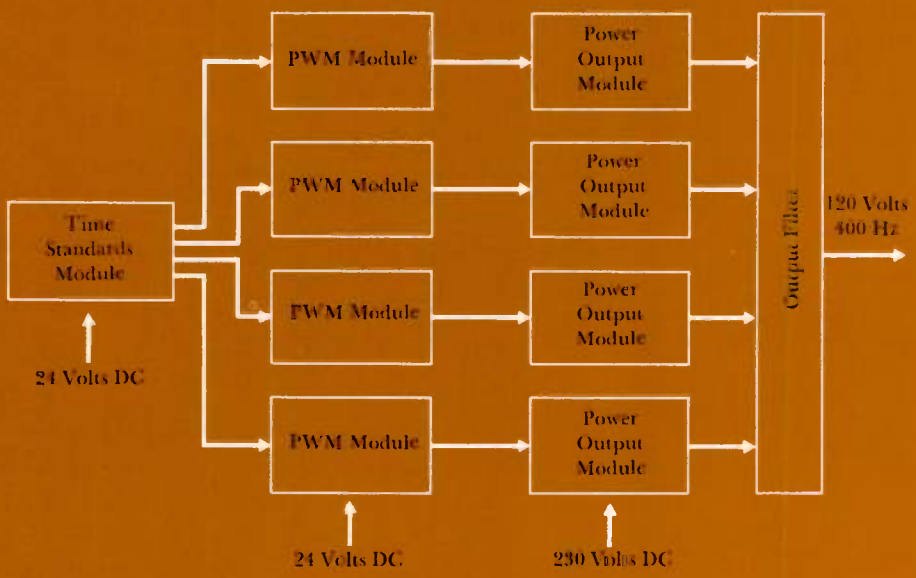

2—Demonstration SPCC inverter is a one-kVA unit with four-phase carrier. Its primary dc power input is at 230 volts; the 24-volt dc inputs supply logic circuits.

filter required. The concept is called staggered-phase carrier cancellation (SPCC). It combines four PWM carrier waveforms that have similar low-frequency modulations, but differing time phases, to synthesize a desired low-frequency waveform at higher voltage.

Since the waveforms used are similar, the low-frequency information (conveyed by the average voltages of each carrier cycle) is similar in each. However, successive waveforms are out of phase by 90 degrees (Fig. 1a). The result, when the carriers are combined, is cancellation of the carrier frequency and much of its harmonic spectrum, while the low-frequency modulation is quadrupled (Fig. 1c). (The low-frequency modulation is the sum of the four PWM waveforms.)

This canceling of the carrier frequency and its harmonics theoretically is complete up to the fourth harmonic, although some lower harmonic content remains in the actual measured outputs of the experimental inverters first built because those units were not optimized. Integrated circuits now being substituted for the relatively crude discrete components first used permit much closer component matching and thereby result in harmonic canceling much closer to the theoretical complete cancellation. The significant harmonics that remain are at high frequency (40 kHz and above), so the filter needed to remove them is small—only a small fraction of the size and weight of the filter for a conventional inverter.

For use as an audio amplifier, the circuitry would be essentially as described for an inverter, but pulse width would be modulated with an audio signal instead of with a constant 400-Hz sine wave. Such an amplifier would be very light for its power output and phenomenally efficient—80 to 90 percent efficient.

The SPCC inverter developed for evaluation has a one-kVA single-phase ac output synthesized by combining four carrier phases (Fig. 2). Its time standards module has a master carrier oscillator and countdown circuits that generate four 10-kHz signals phase-displaced 90 degrees, and a 400-Hz sine-wave oscillator that generates the carrier pulse-width modulating signal. Each carrier

signal, along with the modulating signal, goes to a PWM module followed by a power output module. The PWM modules contain the logic that establishes switching times; the power output modules switch the input power. Outputs from the power output modules to the filter then are four high-power phase-displaced PWM carrier signals. The output filter combines them and filters out all but the desired 400-Hz sine wave.

With presently available power transistors, three-phase 400-Hz sine-wave inverters rated several kilowatts can be built. For still greater system capacity, several inverters could be paralleled.

Products for Industry

Auxiliary pulse relays and dc power supply (clockwise from upper left in photo) are for use with electric utility demand-billing, load-surveying, and load-controlling devices. W-2 interval tripping relay allows synchronization of time intervals from a load-demand recorder to any device that requires a reset pulse of approximately one-third second. It provides two 2-wire output closures from a single 120-volt 60-cycle input contact closure. W-3 isolation relay provides two 3-wire control outputs from a single three-wire input. The relay, using 120-volt 60-cycle input, makes it possible to operate two demand meters or totalizing relays from a single three-wire pulse initiator on a watt-hour meter. It is used to parallel two demand-billing, load-surveying, or load-controlling devices. W-4 polarized relay and W-5 dc power supply, used together, permit transmission of pulses from a three-wire contact device over a two-wire line. Power supply is mounted at sending end, and relay at receiving end. The system is free of errors from contact bounce and momentary interruptions of power supply. *Westinghouse Meter Division, P.O. Box 9533, Raleigh, North Carolina.*

Compact ultrasonic cleaner gives high reliability and performance for cleaning small pieces such as silicon wafers, machined parts, electronic components, and printed circuit boards. The mini-Magnapak cleaner occupies less than one cubic foot; it includes a 1½ gallon stainless steel cleaning tank with magnetostrictive transducers, and a solid-state 20-kHz Magnatrak generator with 200-watt output. *Westinghouse Industrial Equipment Division, 2519 Wilkens Avenue, P.O. Box, 416 Baltimore, Maryland 21203.*

Group control unit provides flexible grouping for ac squirrel-cage motor starters and other control or distribution devices. Called the Type W Jr., it can hold up to four starters with additional panel space for the auxiliary control items needed. Its key advantage is simplified grouped construction as compared with the conventional method of grouping individual controls on a wall with external cable and conduit connections; a single power lead can be brought directly into the enclosure to serve the four control compartments. Available modules include: size 1 or 2, 220/440-volt, 3-phase, either fusible-disconnect switch or circuit-breaker combination line starters; circuit-breaker or fused-disconnect mains and feeders; start-stop pushbuttons; pilot lights; and control circuit transformers with fuse. The unit measures 26 inches high by 32 inches wide by 7 inches deep. *Westinghouse General Control Division, 4454 Genesee Street, P.O. Box 225, Buffalo, New York 14240.*

Test console for dc drive systems makes possible quick and accurate checks of the drive regulator's operation. It is an analog computer unit that can quickly locate any circuit wiring error or tune the regulator for a specific application by simulating such drive-system constituents as generators, motors, and mechanical inertias. It is suited for speed and voltage regulators and certain types of current and tension regulators. The console's meters indicate simulated speed, armature voltage and current, motor field current, and, if applicable, generator field current; they are calibrated in "percent of rated maximum" to eliminate much of the problem of coupling the unit to drives of widely different ratios. *Westinghouse Industrial Systems Division, 4454 Genesee Street, P.O. Box 225, Buffalo, New York 14240.*

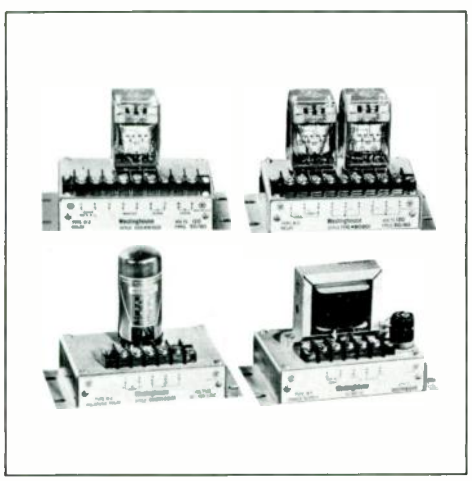

Auxiliary Pulse Relays

Group Control Unit

CORRECTION

A typographical error appeared in an equation in R. F. Cook's article "Residential Electric Heating . . . A Desirable Load for Utilities?", in the November 1967 issue. Equation 1 on page 172, for calculating utility revenues by use of the average and excess demand method, should read:

$$RR_{FA} = \frac{\$/kW}{8760}\left[\frac{\Sigma NCP - SP}{\Sigma NCP - SAL} + \frac{CP\,(SP - SAL)}{CAL\,(\Sigma NCP - SAL)}\right] + PC + \frac{FCC}{(CAL)\,(8760)}$$

About the Authors

Carl R. Olson and **E. S. McKelvy** write about the factors to consider in applying ac motors.

Olson has been applying electrical equipment to processes in the petroleum, petrochemical, paper, metals, and glass industries since joining Westinghouse in 1946. His first permanent assignment after the graduate student course was to the mining, petroleum, and chemical section of the former Industry Engineering Department. In 1964, he moved to the general industries department of Industrial Projects Marketing, where he continues his application engineering work.

Olson earned a BS in EE at Carnegie Institute of Technology in 1943 and an MS in EE at the University of Pittsburgh in 1954. He worked as a plant engineer at the Aluminum Company of America from 1943 to 1944 and then went on active duty in the United States Naval Reserve as a radar officer until 1946. Olson is chairman of IEEE's Industrial and General Applications Group and a past chairman of its Chemical Industry Committee. He has written about 30 technical papers and articles, including one for the *Westinghouse ENGINEER* on power and control systems he developed for electric glass melting.

McKelvy is the petroleum industry representative in the general industries department of Industrial Projects Marketing. He joined Westinghouse in 1941 as a production expediter in the Switchgear Division but then was called into military service, serving in the U.S. Army Air Forces from 1942 to 1945. McKelvy returned to Westinghouse and moved in 1951 to Assembled Switchgear Sales, where he worked on application and pricing of switchgear. He went on to Industrial Sales in 1958 and to the Industrial Systems Division in 1962, working mainly on applying and selecting electrical apparatus for the petroleum industry. He joined Industrial Projects Marketing in 1964.

McKelvy attended Lehigh University and then the Westinghouse technical night school, graduating in 1951. He is a member of the IEEE Petroleum Industry Committee.

Harry G. Lienau, Jerald F. Lowry, and **C. B. Hassan** collaborate in the design and application of electron-beam welders for space, and they have also joined forces to describe the development in this issue.

Lienau is the principal research and development engineer for metal-joining space experiments at the National Aeronautics and Space Administration's Marshall Space Flight Center. He is a member there of a group that is evolving techniques for fabricating space-related structures.

Lienau graduated from Lawrence Institute of Technology in 1942 with a bachelor's degree in mechanical engineering, and he has since done graduate work at the University of Michigan and Western Reserve University. He served as a manufacturing engineer with General Motors Corporation, Ford Motor Company, and Chrysler Corporation before joining the Marshall Space Flight Center in 1960. Throughout his career, Lienau's main interest has been in research and development of the new or improved manufacturing processes and equipment required for new designs and materials.

Lowry graduated from the University of Pittsburgh in 1961 with a BS in physics. He went on to Cornell University, earned his MS in experimental physics in 1963, and joined Westinghouse on the graduate student course. He was assigned to the Research Laboratories, working first on development of electrode materials for solid-electrolyte fuel cells. His later work has been in research and testing of electron-beam guns, design and development of instrumentation and control circuitry for a nonvacuum electron-beam welder, and the space welders described in this issue.

Hassan earned his BSEE at Northwestern University in 1955 and his MSEE there in 1957. He served as a professor of electrical engineering at the College of Engineering, Addis Ababa, Ethiopia, from 1957 until 1960, when he joined Barnes & Reinecke, Inc., in Chicago as an electrical engineer. There he contributed to development of a solid-state ignition system, an automatic motor-generator tester, a solid-state military telephone system, and a solid-state motor controller and precision timer for the U.S. Navy. Hassan then went to the Martin Company, where his work was installation and checkout of Titan-II ICBM electrical systems.

Hassan joined the Westinghouse Research Laboratories in 1963, working first on circuit and package design for a five-kW Navy inverter. He has also contributed to the design and development of power supplies for Navy degaussing systems, and he has been project engineer for a 5- to 200-hp series of Navy static motor controllers as well as for the laboratory and orbital models of the space electron-beam welder described in this issue.

H. E. Lokay obtained a BSEE degree in 1951 from the Illinois Institute of Technology and an MSEE from the University of Pittsburgh in 1956. He joined Westinghouse on the graduate student course and was soon assigned to the electric utility distribution engineering group of the Electric Utility Engineering Department. He was made a sponsor engineer in 1959, working with Midwest electric utility companies and consulting engineering firms on equipment application and systems engineering studies.

In July 1967, Lokay was made Manager of the Generation-Rotating Machinery Section of the Electric Utility Headquarters Department. His group works with Westinghouse divisions and with electric utility companies on engineering and associated problems in the area of power generation.

V. Burtnyk was born in Manitoba, Canada, and received his BSEE degree in 1948 from the University of Manitoba. Upon graduation, he was employed by the Gatineau Power Company, a private electric utility operating in the Province of Quebec, where he worked primarily on system planning and communications.

In 1963, Burtnyk joined Westinghouse as an Assistant Sponsor Engineer in the Electric Utility Engineering Department to work on system studies including power system stability, generation economics, and equipment application problems. He is presently a transmission engineer in the transmission Control and Protection Section of the Electric Utility Headquarters Department.

Emil L. Svensson joined the Westinghouse Aerospace Division in 1954 following a tour of duty in the U.S. Army, where he taught at the Guided Missile School at Ft. Bliss. His initial assignment with Westinghouse was in the Fighter Radar Design Group.

Svensson attended the McCoy College of Johns Hopkins University in the evenings, obtaining his BSE degree in 1960. He began working in television design in 1962 and was the project engineer for the SEC vidicon laboratory camera, the feasibility model for the lunar camera. When work began on the Apollo mission camera, Svensson was responsible for the electrical design group and was subsequently made Technical Director for the project. He is presently responsible for the design of advanced television cameras in the Electro-Optical Systems Section.

Harry R. Sheppard graduated from Carnegie Institute of Technology in 1942 with a BS in Chemical Engineering, and he has since taken graduate work in chemical engineering and chemistry at Brooklyn Polytechnic Institute and the University of Pittsburgh. He spent a year as a chemical engineer with Koppers Company and then moved to Mellon Institute of Industrial Research. Sheppard joined Westinghouse in 1951 in the former Materials Engineering Department. He worked there on development and application of reinforced plastics structures, casting resins, and lightning arrester materials, becoming a supervisory engineer along the way and then manager of the insulation and chemical application section.

Sheppard moved to the Power Transformer Division in 1962 as Manager, Materials and Processes Development Department. His primary interest is in developing functional methods for evolving insulation systems, especially for transformers. He has contributed to the development of glass-polyester track-resistant insulation compositions and cast epoxy insulation structures, and he holds a patent in both those areas of development.

This integrated-circuit logic board is one of hundreds being assembled at the Westinghouse Transportation Center for the Bay Area Rapid Transit train control system. The system will direct trains like those in the background along the 75-mile transit system now under construction in the San Francisco area. The trains will be capable of speeds of 80 miles an hour and can run as frequently as every 90 seconds.